SGP-TR-169

Constant-Pressure Measurement of Steam-Water Relative Permeability

Peter A. O'Connor

June 2001

Financial support was provided through the
Stanford Geothermal Program under
Department of Energy Grant No. DE-FG07-95ID13370
and No. DE-FG07-99ID13763,
and by the Department of Petroleum Engineering,
Stanford University

Stanford Geothermal Program
Interdisciplinary Research in
Engineering and Earth Sciences
STANFORD UNIVERSITY
Stanford, California

Abstract

A series of steady-state experiments have established relative permeability curves for two-phase flow of water in a porous medium. These experiments have minimized uncertainty in pressure, heat loss, and saturation. By attempting to maintain a constant pressure gradient, the experiments have provided a baseline from which to determine the effect of temperature on relative permeability.

The use of a flexible heater with an automatic control system made it possible to assume negligible phase change for the mobile fluid. X-ray computer tomography (CT) aided by measuring in-situ steam saturation more directly. Mobile steam mass fraction was established by separate steam and water inlets or by correlating with previous results.

The measured steam-water relative permeability curves assume a shape similar to those obtained by Corey (1954) for the simultaneous flow of nitrogen and water. Close agreement between the curves by Satik (1998), Mahiya (1999), and this study establishes the reliability of the experimental method and instrumentation adopted in these experiments, though some differences may bear further investigation. In particular, the steam phase relative permeability appears to vary much more linearly with saturation than does the water phase relative permeability.

Acknowledgement

This research was conducted with financial support through the Stanford Geothermal Program under Department of Energy Grant No. DE-FG07-99ID13763.

The contributions of the following individuals are much appreciated:

Glenn Mahiya, for establishing a sound experimental basis and providing information on procedure.

Dr. Kewen Li, for frequent consultation on all facets of the experiment theoretical and practical, and for invaluable experience, knowledge, and insights.

Will Whitted, for truly exceptional technical expertise and assistance in design, construction, and redesign of all the components of this experiment.

Dr. Roland Horne, for patiently providing direction and motivation in the course of this research work.

Table of Contents

Table of Figures

1. Introduction

Single-phase fluid flow through porous media is normally modeled by Darcy's Law. To apply Darcy's Law to multiphase flow requires the addition of the concept of relative permeability, which accounts for effects on the flow behavior of one fluid or phase caused by the presence of another fluid or phase. Relative permeability is believed to depend primarily on the volume occupied by a phase and so is expressed as a function of saturation. Potentially reducing effective permeability by an order of magnitude in some cases, relative permeability can have a dramatic effect on fluid flow and thus is an important parameter to determine in reservoir engineering. The relative permeability relations involving oil, water, and gas are well known and have been established in laboratory experiments. These curves have been used successfully in flow modeling for petroleum reservoir engineering.

Geothermal reservoirs engineers are necessarily concerned with the flow of steam and water; steam-water relative permeability curves have been difficult to produce due to the inherent phase changes between the fluids and the uncertainty of determining water saturation. A series of experiments conducted by the Stanford Geothermal Program have sought to establish steam-water relative permeability relations; these experiments have maintained near-adiabatic steady-state conditions, determined saturation through X-ray computer tomography, and accounted for slip factor and capillary end effects.

The current work followed on results obtained previously. The objective was to remove any potential effect of temperature on relative permeability by maintaining a constant pressure and temperature gradient for every stage of the experiment. Further, the high pressure gradient should give more reliable and reproducible results with less error than a low pressure gradient. The results were compiled and analyzed by several methods, presenting a comprehensive data set.

2. Background

2.1. Relative permeability

Relative permeability describes the effect of one fluid or phase on the flow behavior or another fluid or phase. Fluids interfere with each other by occupying pore volume, limiting connectivity, and causing effects of interfacial tension. These effects can be measured quantitatively and determined by including a relative permeability parameter, which is the permeability to a given fluid of a porous medium partially saturated with another fluid. Relative permeability is expressed as a ratio of this permeability over the medium's measured absolute permeability, and so generally is a number between 0 and 1. Relative permeability is primarily a function of saturation but could also have some dependence on temperature, pressure, or flow rate. For multiphase flow of steam and water the mass flux for each phase is not constant since one phase can be readily transformed to the other. The current experiment has been designed to minimize phase changes by maintaining adiabatic conditions.

Relative permeability relations for oil, gas, and water have been used extensively in petroleum reservoir engineering, but steam-water curves are not as well established. The curves developed by Corey (1954) for gas-oil relative permeability, and the simpler linear relations ("X-curves"), are the most commonly used forms of relative permeability relations.

The Stanford Geothermal Program has conducted many experiments to determine steam-water relative permeability relations. The experimental procedure has been developed and enhanced over time to ensure greater accuracy and more rigid experimental controls. These experiments have found linear curves in some cases and Corey-type curves in others. Steam relative permeability has been seen to be a more linear function of saturation than is water relative permeability, though the apparent magnitude of this difference has varied.

Single-phase flow in a porous medium is typically governed by Darcy's law relating the fluid velocity, u, to the pressure drop, ΔP, over the distance, ΔL; the viscosity, μ, and; the absolute permeability, k, of the medium as in Equation 2.1.

$$u = \frac{k}{\mu}\frac{\Delta P}{\Delta L} \quad \textbf{(2.1)}$$

In the case of two-phase flow, we introduce the relative permeability k_r as in Equation 2.2:

$$u = \frac{k_r k}{\mu}\frac{\Delta P}{\Delta L} \quad \textbf{(2.2)}$$

To determine permeability from a mass flow rate m, and considering multiphase flow of steam and water, we use Equation 2.3. The cross-sectional area of the porous medium is A, and the density of water and steam are ρ_w and ρ_s, respectively:

$$m_w = \frac{k_{rw} k A \rho_w}{\mu_w}\frac{\Delta P}{\Delta L} \quad \textbf{(2.3a)}$$

$$m_s = \frac{k_{rs} k A \rho_s}{\mu_s}\frac{\Delta P}{\Delta L} \quad \textbf{(2.3b)}$$

The total mass flow rate is m_t, and the steam quality is x. Then we can rearrange the equations to solve for k_{rw} and k_{rs} as follows:

$$k_{rw} = \frac{(1-x) m_t \mu_w}{k A \rho_w}\frac{\Delta L}{\Delta P} \quad \textbf{(2.4a)}$$

$$k_{rs} = \frac{x m_t \mu_s}{k A \rho_s}\frac{\Delta L}{\Delta P} \quad \textbf{(2.4b)}$$

2.2. Saturation

Saturation, the fraction of pore volume occupied by a given phase, was determined in this experiment by use of X-ray computer tomography (CT). This has made determination of in-situ steam saturation considerably easier than was the case for previous experiments. The CT number is directly related to the density of the material being scanned, with a higher value indicating a denser composition. Therefore, steam-saturated porous media show a lower CT value than water-saturated porous media.

First, a porosity distribution can be calculated by scanning the rock once when it is dry and again when it is saturated with cold water, determining CT_{dry} and CT_{wet}. Using the known values CT_{water} = 0 and CT_{air} and -1000, we apply Equation 2.5 to determine the porosity distribution:

$$\phi = \frac{CT_{wet} - CT_{dry}}{CT_{water} - CT_{air}} \tag{2.5}$$

Then, we establish reference values of the CT values along the core for complete steam saturation and for complete hot water saturation. From this point, at any later measurement where we have a CT value for two-phase flow, it is a simple interpolation to determine the exact saturation, by Equation 2.6. Note that it is important to use the CT value for hot water rather than that for cold water, since there is a density change between the two. In this case, the initial imbibition step involved flowing superheated steam into an evacuated core. This served as the first flow test as well as fixing the steam saturation values.

$$S_{st} = \frac{CT_{hw} - CT_{meas}}{CT_{hw} - CT_{steam}} \tag{2.6}$$

$$S_w = 1 - S_{st} \tag{2.6}$$

2.3. Slip factor

Gases flowing under pressure experience a higher effective permeability than liquids do; the permeability of a porous medium measured by flowing single phase gas varies with the average pressure in the medium. This effect is known as Klinkenberg effect, and it is accounted for by correcting gas relative permeability with a slip factor. The correction is shown in Equation 2.7, where *b* is a value of 6.58 psia as determined by Li and Horne (1999).

$$k_{rs(corrected)} = \frac{k_{rs}}{\left(1 + b/p_m\right)} \tag{2.7}$$

2.4. Overview of previous results

As mentioned, relative permeability experiments at Stanford have been progressing for several years with successive improvements to the apparatus and procedure. The effectiveness of the experimental procedure was greatly increased with the employment of a CT scanner to determine steam saturation (Clossman and Vinegar, 1988). The recent experiments most carefully considered were those of Ambusso (1996), Satik (1998), and Mahiya (1999). Each experiment introduced new controls and mechanisms to ensure optimal experimental conditions and accuracy. Ambusso (1996) employed real-time measurement of temperature and pressure to determine the status of the core at several points along the core. Ambusso conducted his experiments at a range of temperature and pressure gradients. Temperature at the first core thermocouple ranged from 101 °C to 117 °C. The fluid was injected in two-phase flow by heating it under pressure and then flowing it through a throttle valve. Ambusso (1996) determined an X-curve relationship between relative permeability and saturation. Experiments by Satik (1998) changed the inlet mechanism, adding separate inlets for steam and for water. Mobile steam quality was calculated on the basis of separate inlet fluid flows and measured heat flux out of the core. A new core was prepared, with a core holder of high-temperature plastic. Satik's results indicated a Corey-type curve relationship for steam-water relative permeability, with a steam residual saturation of less than 10% and a water residual saturation of 30%. A subsequent experiment by Mahiya (1999) solved the problem of phase changes with the addition of a flexible heat guard. This maintained adiabatic conditions throughout the experiment. Mahiya's experiment relied on a combination of separate inlets and enthalpy calculations to determine the steam quality. Generally, mobile saturation during the imbibition steps could be determined by maintaining single-phase flow from each inlet, while some of the high-water-saturation drainage steps required mixed flow from each inlet with the actual mobile saturation estimated from enthalpy. Mahiya's results generally agreed with Satik's, though the steam relative permeability values were slightly higher and the intersection of steam and water relative permeability was at $S_w = .65$ rather than $S_w = .55$. Mahiya also concluded that there was a Corey-type relationship.

3. Experimental Design

The experimental design used in this experiment built on the advances in procedure and apparatus developed in the previous experiments.

3.1. General design and apparatus

The experiment determined the steam-water relative permeability for a Berea sandstone core. This was the same core used in experiments by Satik (1998), Mahiya (1999), and Belen (1999). The core had the following properties: length 43 cm, diameter 5.04 cm, measured porosity 24%, and permeability 1200 md. Clays in the core were deactivated in previous experiments by baking it at 800 °C, and the core was cemented with epoxy to a core holder of high-temperature plastic.

Pressure ports were drilled through the core holder at fixed intervals; heat-resistant plastic tubing ran from these ports to a pressure transducer box. At these ports, as well as the inlets and outlets, the pressure tubings were fitted with T-type thermocouples. There were eight pressure and temperature measurements along the core, two at the inlets, and one at the outlet. A flexible heat guard, described in Section 3.3, was wrapped around the core holder. A heat flux sensor was fixed under every section of the heat guard, sending both heat flux and temperature data to the system. As these sensors were outside the core holder, they did not register the interior core temperature as accurately as did the thermocouples at the pressure ports. The whole core was wrapped with insulating fiber on top of the heat guard to further minimize heat loss. A schematic of the apparatus is shown in Figure 3.1, and a photograph is shown in Figure 3.2.

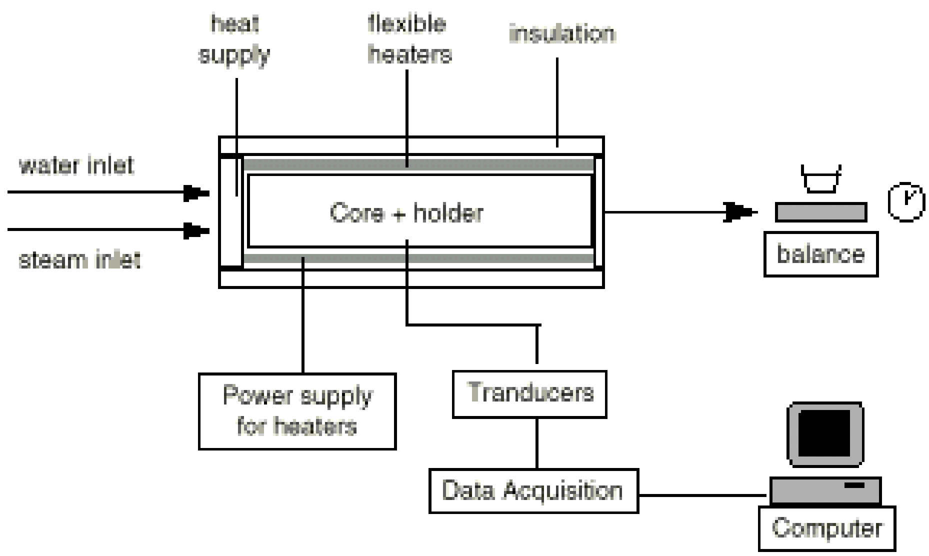

Figure 3.1: Experimental design schematic.

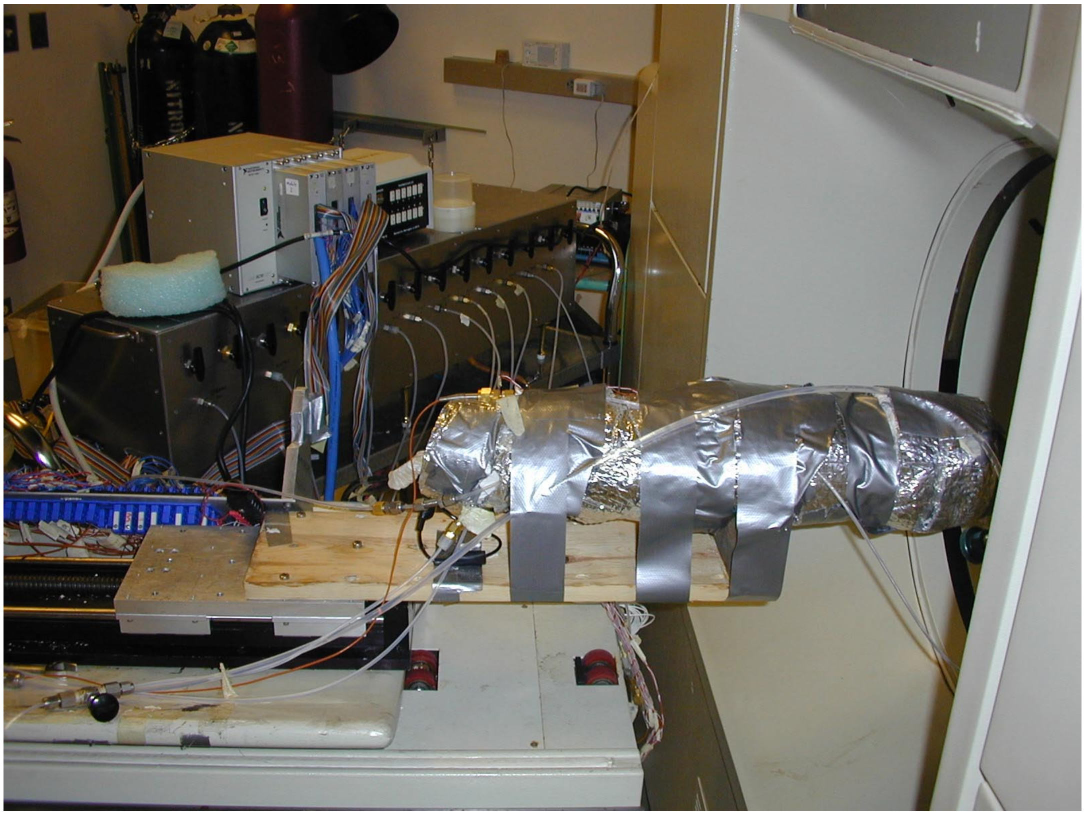

Figure 3.2: Core assembly mounted on CT scanner couch. Pressure transducer box and SCXI modules and chassis box seen in background.

The outlet end piece was plastic, fitted with a pressure port and thermocouple. The inlet end piece was stainless steel, fitted with two pressure ports and thermocouples, one for the steam inlet and one for the hot water inlet. A thermal switch was installed within the end piece to deactivate the furnaces in the event the end piece temperature exceeded 170 °C. This was added to prevent damage to the core in the event of interruption of water flow to the heaters, as had happened in previous experimental attempts.

Deionized distilled water was sent to a boiler, where it was deaerated. The boiling water was then pumped through a cooling tank to enable it to pass through the displacement pump and into the inlet end piece. Two resistance heaters heated the water either to liquid just below the saturation temperature or to vapor just above the saturation temperature, and the fluids then entered the core and mixed. A tube ran from the outlet to a collecting flask on a scale, where the outlet mass flow rate could be measured and compared to the inlet mass flow rate to determine if the system was at steady state.

3.2. Data acquisition system

We recorded pressures, temperatures, and heat fluxes with a data acquisition system designed for previous experiments. This system utilized several National Instruments devices to process a considerable amount of data simultaneously and display it in an easily readable format on a PC. Signals from the transducers, thermocouples, and heat flux sensors were sent through a patch board to SCXI-1100 modules, and these modules were installed in a SCXI-1000 chassis box. The chassis box sent the data to a PC, where the data was displayed. The PC ran the National Instruments program LABVIEW version 4.1, a graphical programming utility for instrumentation. LABVIEW provided a means of monitoring heat flux, temperature, and pressure simultaneously, as well as controlling the flexible heaters. LABVIEW did not monitor the flow rates or furnace settings directly, but these could be entered manually so that they would be saved with the pertinent data. We reconfigured previous LABVIEW routines to suit the needs of this experiment.

3.3. Flexible heaters and control protocol

A flexible heat guard consisting of 18 independent heating elements was wrapped around the core. A schematic is shown in Figure 3.3. The flexible heaters were connected through a step-down transformer to a variable output power supply. A LABVIEW routine was redesigned to activate the heater units as necessary to maintain a constant heat flux of near zero. To control the individual heaters, we used National Instruments' SCXI 1163-R module, consisting of 32-channel optically isolated digital output/solid-state relays. In the closed state, each relay had a maximum resistance of 8 ohms and carried up to 200 mA of current. A LABVIEW algorithm was constructed to monitor the heat flux and adjust the heaters as necessary to maintain adiabatic conditions. As the relays are not variable voltage controllers but simple on/off switches, the necessary heat flux was generated by setting a duty cycle to each relay, and thus to each heater. A duty cycle of 0% corresponded to relay being closed and the heater operating all the time, while a duty cycle of 100% corresponded to the relay remaining open and the heater being inactive. A cycle in between would open the relay a percentage of the time equal to the duty cycle during each period. The heaters were generally set to a cycle period of 2-3 seconds, and the ideal power setting was to have most of the duty cycles near 50%.

The control protocol checked the heat flux every minute. If the heat flux for a specific heater was outside the tolerance range, usually 30 W/m^2, the program would increase or decrease the duty cycle accordingly by a given increment, typically 5%. Due to PC speed and memory constraints, this protocol often failed to work properly when the graphical displays were active. For this reason, the control protocol was allowed to establish the correct heater settings for adiabatic conditions, then the duty cycle increment was set to 0% and the graphical displays were activated. If the heat flux averages left the tolerance range, the control protocol would be reengaged to adjust as needed. In some cases, when specific heat flux sensors failed to function adequately, the duty cycle of a given heater would be set manually to equal that of the heaters on either side and preventing from adjusting independently.

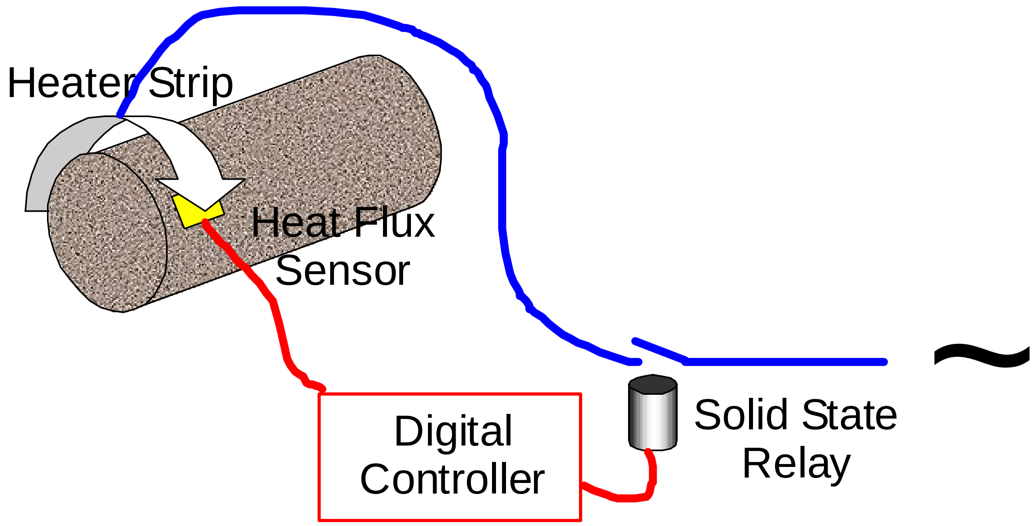

Figure 3.3: Flexible heat guard design.

3.4. CT scanner

A modified medical X-ray CT scanner was employed to determine the water saturation at all points along the core. In-situ saturation values were calculated from images generated by the Picker Synerview 1200X X-ray CT scanner. The core assembly was mounted and secured on a couch, which could be controlled by the console on the scanner. The scanner was equipped with a visible laser and a digital display of the couch position. We therefore could establish accuracy of the measurement by ensuring that each scan was at the same relative position along the core for each experiment.

The scanner had been augmented and modified to fit the needs of petroleum and geothermal reservoir engineering experiments, in particular with the addition of a large range of variable power settings. This experiment required setting the scanner at 125 kV, 65 mA, an exposure time of 8.49 seconds per slice, and a slice thickness of 10 millimeters. The large slice thickness of the CT scans reduced any potential errors caused by inaccuracy in the couch positioning system.

3.5. Suggested future design modifications

This experiment provided insight into potential future improvements to the experimental procedure and apparatus. The data acquisition system is exceptionally useful and should become even more powerful and adaptable with newer versions of LABVIEW. We suggest employing a faster PC to take full advantage of LABVIEW's capabilities. The CT scanner is accurate and provides a clear picture of the interior of the core. The flexible heat guard greatly enhances the effectiveness of the experiment by negating the need for heat loss estimations.

The core holder itself could be improved, in particular the inlet end piece. The stainless steel end piece is resistant to thermal damage and permits the addition of a thermal switch to prevent damage to the core. However, this particular device creates difficulties in controlling the steam and water inlets. Excess heat from the steam furnace heats the inlet water, to the extent that it was often not needed to supply any heat at all to the water furnace in order to have water at the saturation temperature. Maintaining superheated steam and liquid water at the two inlets was difficult. At times, the hot water temperature appeared to exceed the saturation temperature, despite the fact that there was not enough power going into the core to heat the given flow rate to superheated conditions. This may have been a consequence of steam pockets forming in the water furnace at the location of the thermocouple, or asymmetrical water flow around the furnace. In all of these cases, the temperature at the first pressure port was at the saturation temperature, even if both steam and water inlets had appeared to be injecting superheated steam. Therefore, it is not considered that injection through then water inlet was actually superheated steam in these cases.

The steel end piece also at times heated the water at the first pressure port to a higher temperature than the water in the inlet. This would be the case when the energy produced by the heaters could not be entirely transferred to the injected fluids as they passed through the end piece. This effect is visible in a couple of the temperature profiles in Section 5, though it was often a problem that had to be fixed during the experiment. If, as a consequence of heat transfer between the furnaces, there was more steam entering the core than was entering solely through the steam inlet, we would have underestimated the steam relative permeability in some cases.

A future end piece should retain the stainless steel construction, but should have a greater separation between the steam furnace and the water furnace. A gap cut down the length of the endpiece, filled with insulation or left open to the air, would greatly reduce heat transfer between the steam heater and the water heater. A thermal switch should be installed in the steam heater side of the inlet, since it will be necessary to deactivate the heaters in the event of interruption of water supply. Two other methods might allay the problem of heat transfer between the heaters. Preheating the steam would reduce the power necessary for the steam furnace, as would the use of external furnaces. The internal furnaces minimize atmospheric heat loss, an advantage that we may not wish to dispense with.

The displacement pumps used in this experiment were accurate, but not very reliable. In one case, loss of fluid flow resulted in damage to the core and warranted the installation of the thermal switch. After that modification, there were several other flow decreases that caused temperature spikes and triggered the thermal switch. We suggest replacement of the displacement pumps.

If the experiment is to be repeated at a different pressure gradient, additional modifications would be necessary. The current core holder is probably not suitable for temperature and pressure gradients significantly higher than those used in this experiment. A titanium core holder might be an effective option if its cost is not prohibitive.

4. Experimental procedure

This section describes the steps taken in the experiment, conceptual goals, and challenges encountered. The experimental procedure closely followed the procedure established by Mahiya (1999), though certain changes were made to enhance the effectiveness of the experiment.

4.1. General procedure

The water supply was set up as detailed in Section 3. The boiler had to be refilled periodically with water and allowed to boil for a length of time sufficient to deaerate the water. Once the water was deaerated and the boiler was full and turned off, the system could generally be allowed to run overnight or for several hours during the day to establish steady-state conditions. This was not the case for experiments at high mass flow rate. Outlet water was collected occasionally and weighed on a scale to compare the outlet mass flow rate to the injection mass flow rate, to verify steady-state conditions and to confirm the accuracy of the pump flow rates.

The experiment began with an imbibition process. Performing the imbibition process first allowed determination of the maximum necessary steam flow and correspondingly the maximum necessary power input. The initial step was a flow of superheated steam into an evacuated core; as the CT values for this step were actually slightly lower than those found for the evacuated core, this was used as the baseline for calibration of the CT values. Therefore, the steam saturation in this step was taken to be 100%, as the temperature at all points along the core was considerably higher than the saturation temperatures. Fluid injection continued, with an increasing water mass fraction in each successive step of the experiment. We attempted to control temperature sufficiently that there was obviously single-phase flow from each inlet. At each step, after the system had reached steady-state conditions, a CT scan of the core was taken. The images were processed on the Picker console, transferred to a magnetic tape drive, and then saved to a PC.

Once the imbibition step was complete, the drainage process began. During this process, only one inlet pump was available and two-phase fluid was injected at saturated conditions. Mobile steam quality was calculated as detailed in Section 5.3. The drainage experiments took place over a range of high and moderate water saturations. Unfortunately, it was not possible to further investigate the region of low water saturation.

4.2. Constant pressure gradient

In this experiment, we attempted to maintain a constant pressure gradient of 0.89 psi/inch (a 15 psi pressure drop over a 43 cm core) to avoid any effects of temperature on relative permeability. The outlet was at atmospheric pressure, and an inlet pressure of 15 psig corresponded to a saturation temperature of 120 °C. Constant pressure gradient was to be maintained by varying the flow rate as needed. Total mass flow rate ranged from 2 g/min to 16 g/min for all of the steps at the target pressure gradient.

4.3. Procedural limitations

Certain modifications to the experiment were necessitated by limitations of the apparatus. During the drainage step, hot water was to be injected through one inlet and steam through another, as had been done in the imbibition step. However, in this stage of the experiment we sought to produce very small steam flow rates, to further examine the area of high water saturation. For the flow rates considered, it proved to be impossible to heat fluid in the steam inlet to superheated conditions without considerable transfer of excess heat to the core and to the hot water inlet. It proved easier to produce miniscule amounts of steam by heating the inlet water to the saturation temperature. Later in the drainage step, it would have been possible to return to a dual-inlet setup, but the other displacement pump had begun to fail, possibly due to a leaking seal.

The original inlet thermocouples failed and were replaced before the drainage step, but the replacement thermocouples were less accurate due to difficulties in positioning them precisely enough. They routinely read temperatures too high (if the thermocouple was positioned near the heater) or too low (if it was further back along the pressure tubing).

In the drainage step, the temperature at the first pressure port was used to determine if the flowing fluid was at saturated conditions. While it would be better to know the actual inlet temperature, it was not crucial, as we did not have separate inlets of superheated steam and liquid water.

Certain of the drainage steps may not have reached steady-state flow. Due to the large volume of water involved, they could only be left unattended for 2-3 hours at most before the boiler would need to be refilled; as a consequence, they could not stabilize overnight. In these cases, they were monitored and as much time as possible was allowed for the system to stabilize. This most likely accounts for the saturation front seen in some of the drainage experiments.

5. Experimental results and discussion

5.1. General Results

A total of 28 steady-state experiments were performed over a period of several weeks. The resulting data covered the full range of saturations, with particularly large amounts of data for regions of moderate saturation. Fifteen imbibition experiments were performed, followed by 13 drainage experiments. The drainage experiments had greater success in covering the range of high water saturations but suffered from loss of accuracy in determining the flowing steam saturation. Near-adiabatic conditions were maintained for all experiments. Other than an initial flow of 100% steam into an evacuated core, the maximum steam saturation reached was about 65%. The maximum water saturation reached was 100%, due to condensation of immobile steam during the earliest drainage step. The full results of the experiment are presented in Appendix B, in chronological order.

5.2. Saturation

Saturation profiles during the imbibition step, shown in Figure 5.1a, were constant across the core and cover the range of steam saturation from 30% to 65%. These tests did not cover a range of high-water or high-steam saturations. The saturation profiles in the drainage step, shown in Figure 5.1b, exhibit greater variation across the core, but also covered a wider range of saturations. The existence of a saturation front and multiple flat saturation regions allowed these experiments to provide useful data. The presence of fronts in the drainage phase may be the result of unsteady-state conditions, or it may be the result of the steam in the latter part of the core being more difficult to displace. In results presented later in this chapter, one relative permeability graph is presented using the average saturation from the first half of the core, which showed stable saturation at all points. Capillary end effect was visible in many of the steps. For this reason, one relative permeability graph is presented excluding the pressure ports nearest to the inlet and outlet.

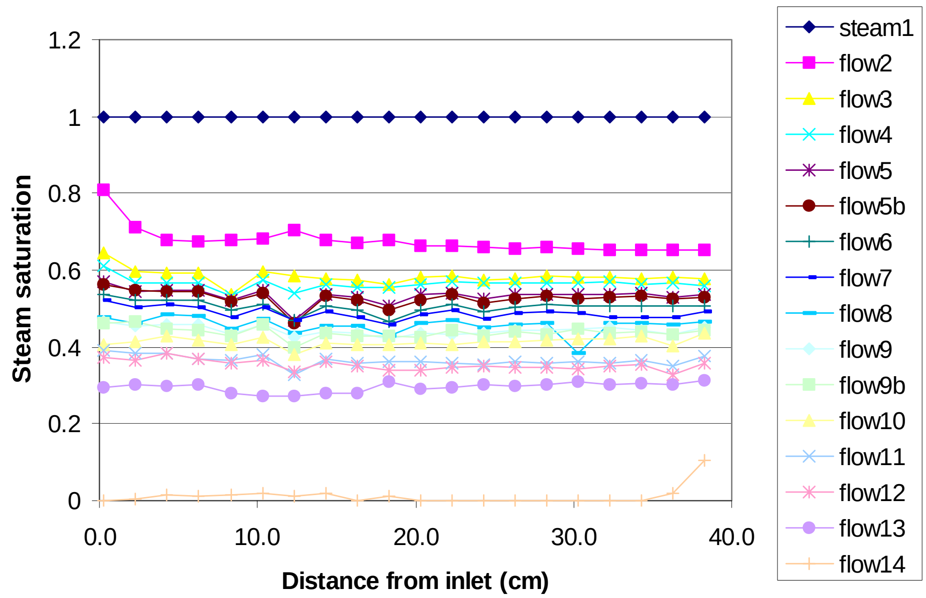

(a) Imbibition

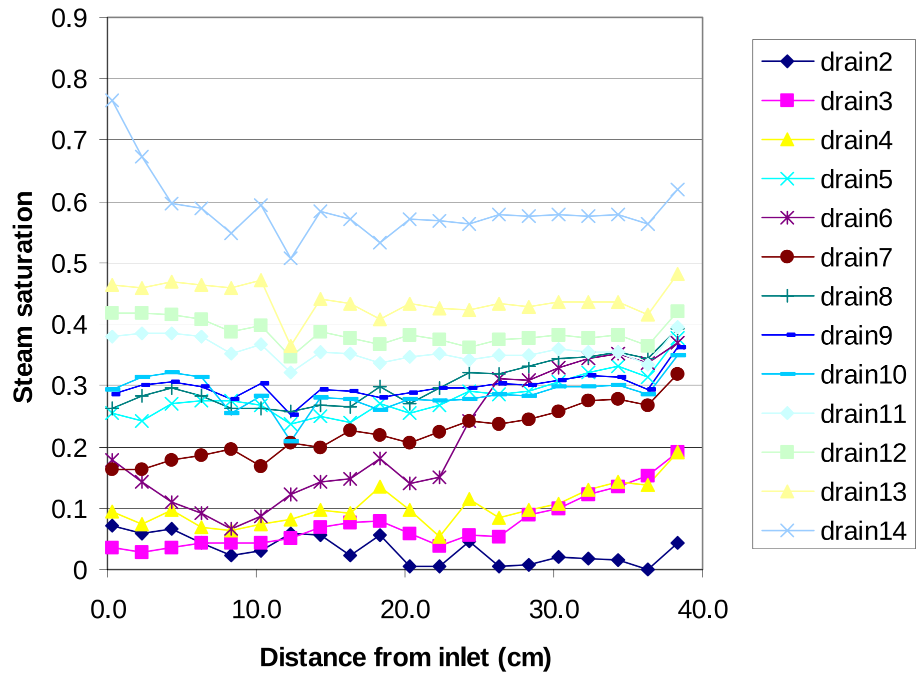

(b) Drainage

Figure 5.1: Saturation profiles.

5.3. Correlation between mobile and in-place saturation

For the drainage steps, only one inlet could be used. This was generally acceptable for determining the liquid flow rate when the total mass flow rate was large, as it was in most of the drainage steps. It was necessary to determine the steam flow rate for these experiments and both flow rates for the low mass flow rate drainage experiments. Analyzing previous flow tests from this experiment, and considering other experiments, we derived a reasonable correlation between inlet steam quality and in-place saturation. It appears that large amounts of inlet water can displace even "immobile" steam saturation, though this may be a factor of a phase change too minor to be prevented by the heat guard. These correlations are shown in Figures 5.2a and 5.2b. A relationship was derived and applied to the data, estimating the inlet and mobile steam quality from the mean saturation. Equation 5.1a was used for high steam saturation, (S_{st}>.20) and Equation 5.1b was used for lower steam saturation. In this manner, steam inlet quality was calculated for the drainage steps. We present this method with some reservations, but consider the uncertainty in steam flow rate to be moderate and the uncertainty in water flow rate to be extremely minor. As an example, underestimating a steam quality of 6% as being 3%, a 50% error, would only result in overestimating the water mass flow rate by 3.2%. In most cases, the estimated steam quality was considerably less than 1%.

$$x = \frac{S_{st} - 0.3886}{0.2462} \tag{5.1a}$$

$$x = e^{\frac{Sst - 0.5225}{0.0415}} \tag{5.1b}$$

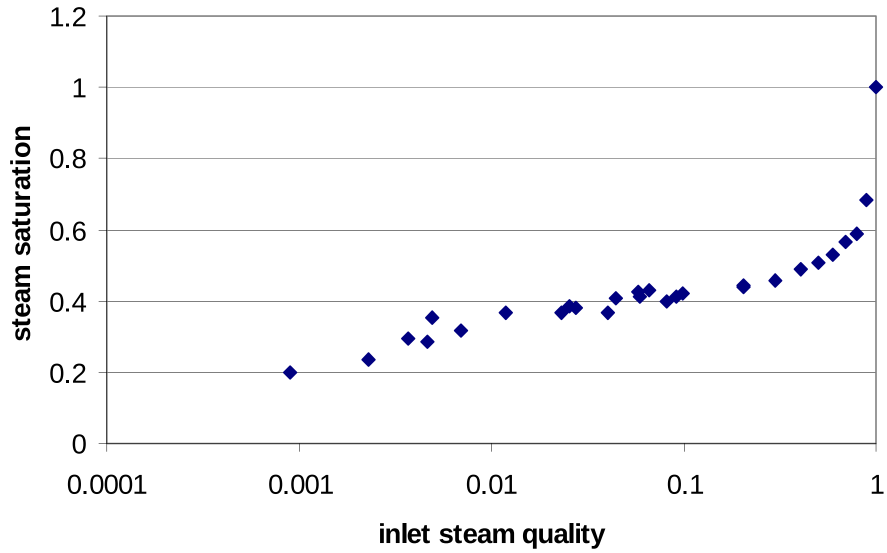

(a) Logarithmic plot

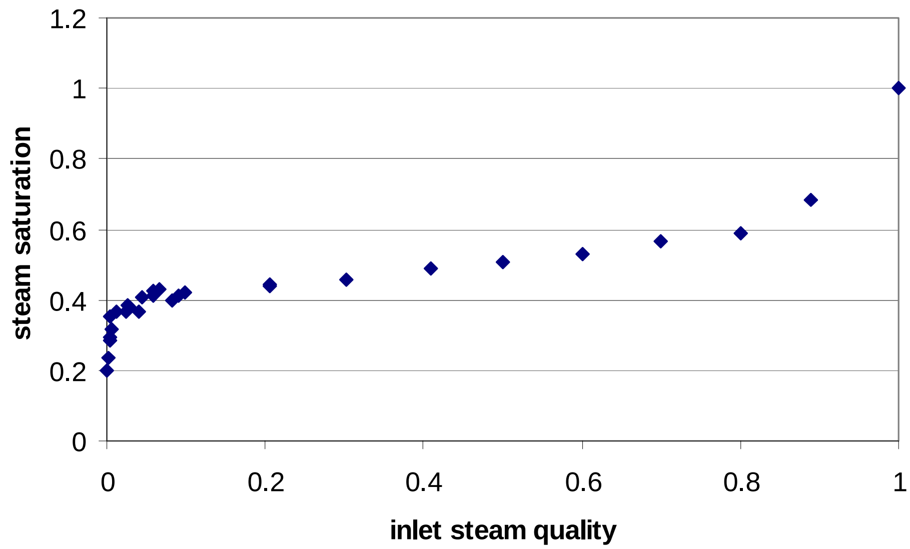

(b) Linear plot

Figure 5.2: Correlation of saturation with inlet quality.

5.4. Pressure

The goal of this experiment was to maintain a constant pressure drop of 15 psi by varying the flow rate as needed. This was successfully accomplished throughout the entire imbibition phase, save for the 100% water inlet step at the end. The constant pressure gradient could not be maintained in a few cases of high water flow, such as the end of the imbibition phase and the first few trials of the drainage phase. In these cases, the pump and heater could not supply sufficient water at 120 °C to maintain a 15-psi pressure drop across the core. For attempts to increase the flow rate further, the main limitation appeared to be the rate of heat transfer from the water heater to the fluid flowing over it. The water being injected remained considerably below the saturation temperature, yet the temperature at the first pressure port was higher than that measured for the hot water inlet. This indicated that the heater was not transferring all of its heat to the fluid, and that the excess was transferred directly to the core, which could result in damage to the core. Pressure profiles are shown in Figure 5.3a and Figure 5.3b. Note that the pressure drop is very close to 15 psi for most of the drainage steps and all but one of the imbibition steps.

A second reason to maintain the 15 psi pressure drop is that it appears the transducers are most reliable in that range. Flow tests at lower pressure seem more likely to have minor anomalies, which resulted in relative permeability either inflating or becoming negative. This may simply be a consequence of absolute errors and fluctuations in the pressure readings, which produce a greater relative effect at low pressure. For this reason, the flow tests with lowest pressure gradients are excluded from most presentations of the relative permeability data.

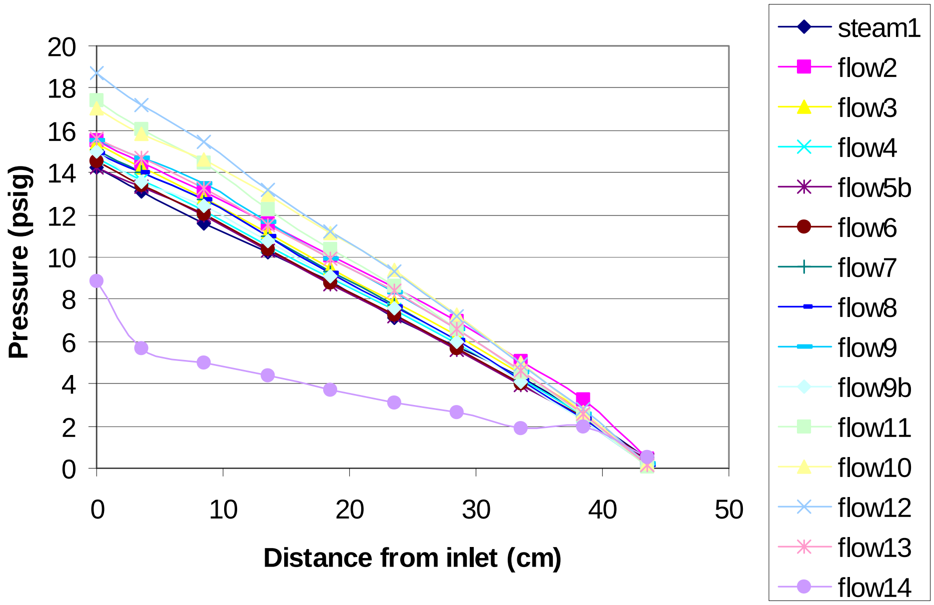

(a) Imbibition

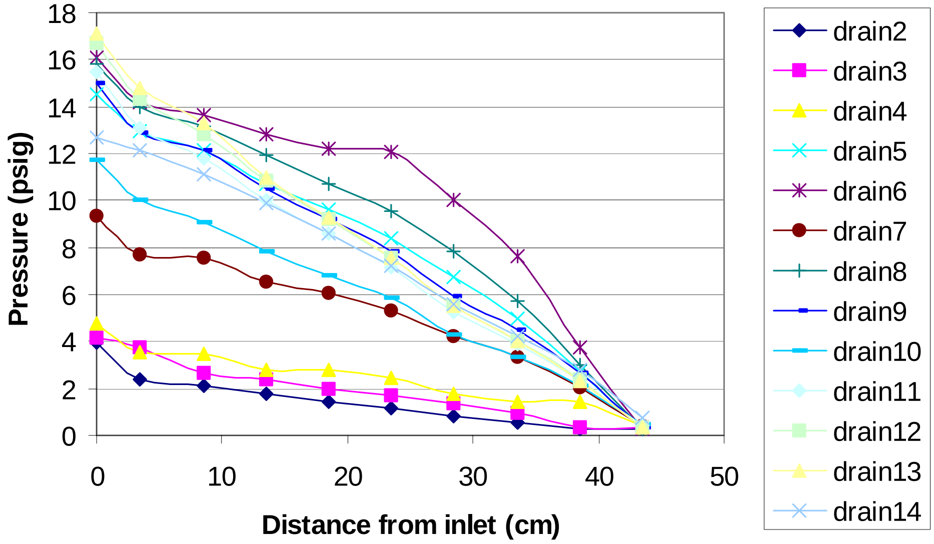

(b) Drainage

Figure 5.3: Pressure profiles.

5.5. Temperature

The core temperatures generally matched the saturation temperatures at the measured pressures. Slight deviations due to instrument inaccuracy and fluctuation existed, so we took 1 psi to be an acceptable margin of error between the measured temperature and the saturation temperature. Anything outside of that range was considered superheated or unsaturated. Some steps, such as the steam imbibition phase, exhibited a higher temperature at the first pressure port than at the inlet. This was regarded as a consequence of inadequate heat transfer away from the steam heater, with the result being that the heater was radiating excess heat through the end piece and into the core. This was generally not a desirable condition. Temperature profiles are shown in Figure 5.4a and Figure 5.4b. Note that for much of the drainage phase the thermocouples near the end of the core were not functional. The more reliable thermocouples from the end of the core had been moved to replace malfunctioning thermocouples at the inlets, as controlling the inlet temperature as precisely as possible was of greater importance than monitoring the outlet temperature.

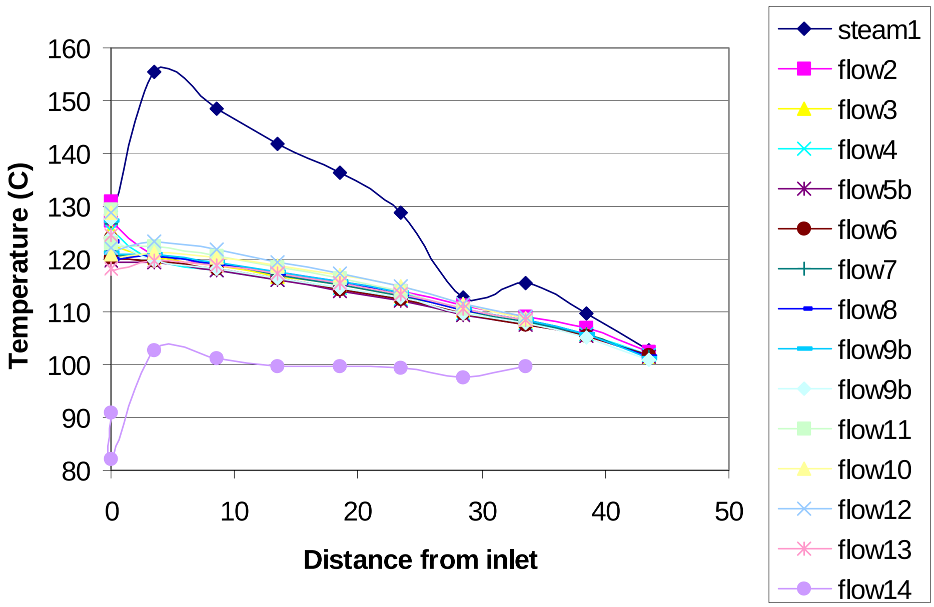

(a) Imbibition

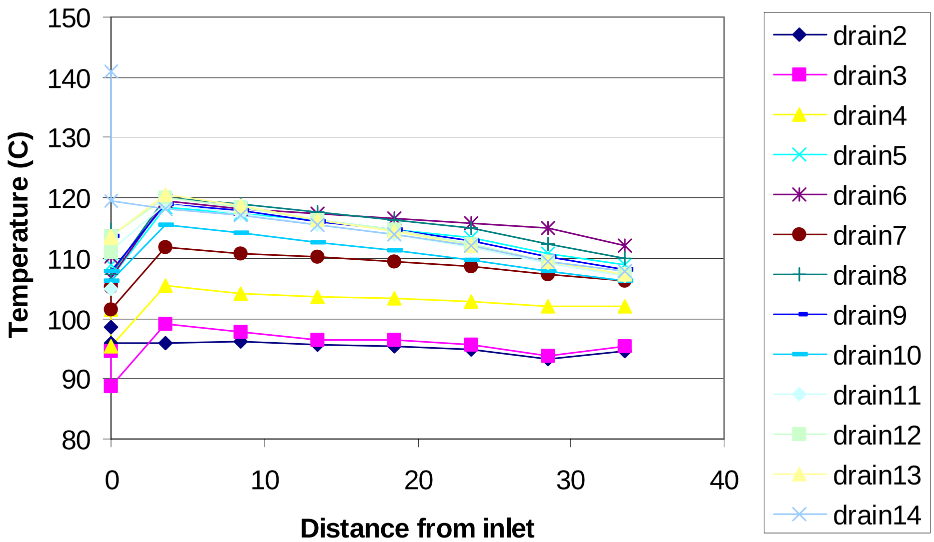

(b) Drainage

Figure 5.4: Temperature profiles.

5.6. Heat flux

The average heat flux was kept within 30 W/m^2 of a target heat flux of 0 W/m^2 throughout each experiment. As the individual heaters cycled on and off, the instantaneous heat flux at any given sensor at a specific time may have been between 80 and -80 W/m^2. The instantaneous heat flux data was recorded but is not an effective measure of the actual heat flux and so is not included here. Two heat flux sensors were highly erratic, so the heaters for these strips were set to the duty cycles of adjacent heaters. A recurring concern throughout the experiment was heat flux through the stainless steel inlet end piece. This prevented the calculation of inlet enthalpy based on power supplied to the furnaces, which would have otherwise been a useful method to estimate inlet steam quality.

5.7. Relative permeability

Results for relative permeability appear to be Corey-type curves for water and possibly a more linear relationship for steam. Maximum steam saturation appears to be around 70%, and maximum water saturation appears to be 90%. When considering the flow trials not occurring at the target pressure gradient, there are indications that k_{rw} may be as high as 0.65 or even higher. These less-reliable trials comprise nearly all of the cases with water saturation greater than 0.8, so it might not be appropriate to discard them entirely.

In all figures other than Figure 5.7 (the harmonic averages), the data from the first pressure port and the outlet are excluded. Each stage of the experiment showed a considerable disparity between the data from these ports and the data determined elsewhere along the core. This was most likely due to capillary end effect or unusual pressure behavior involving the placement of the inlet and outlet pressure tubings. The data are presented as follows:

Figures 5.5a and 5.5b show the relative permeability curves for all data points other than the first pressure port and the outlet. Note that a few data points indicated permeabilities significantly greater than 1 or less than 0 even after correcting for the slip factor; these were attributed to instrumentation anomalies and were ignored. Figure 5.5b focuses on the data near the area of low permeability around S_w = 0.64. In this view, we see that the imbibition steps show scattered clusters of the k_{rs} data, rather than any significant trend.

Figures 5.6a and 5.6b show the relative permeability for all points in the interior of the core (pressure ports 2-7) and the points from flow tests with a gradient less than 12 psi. This shows a maximum water saturation of 0.92, a maximum steam saturation of 0.69, and increasing scatter in k_{rw} as S_w increases.

Figures 5.7a and 5.7b show the mean relative permeabilities across the core for each step; Figure 5.7a shows the mean values from all steps, while Figure 5.7b excludes the runs which did not occur with a pressure drop near 15 psi.

Figures 5.8a and 5.8b show the relative permeability calculated at the data points 2-5, which had uniform saturation in each flow test and were generally free from anomalous pressure readings resulting in inflated or negative relative permeability. Figure 5.8a shows all the data, and Figure 5.8b shows the averaged values for each flow test. These graphs exclude the flow tests of high water saturation that had a pressure drop of less than 12 psi. The corrections show some improvement in the scatter for the graph of all data points, but no real change from the harmonic means of the entire core.

Note that there are considerably more data points than there are steady-state experiments; each experiment allowed determination of relative permeability across every interval between pressure ports. In addition, some experiments had pressure and temperature data recorded several times during the 30-minute scanning interval, resulting in multiple relative permeability values for a single flow test if there was variation in the transducers or thermocouples.

It is our conclusion that the data from the harmonic means (Figure 5.7a) are the most reliable and the best representation of the total data gathered. It then appears that while water relative permeability follows a Corey-type curve similar to that found in previous experiments, steam relative permeability follows a steeper and more linear trend. This conclusion does not change when different sections of the data are considered. The steam relative permeability deviates from a Corey curve in several regions, and not simply for the drainage data points involving a mobile steam quality calculated through correlations. It may be that steam relative permeability follows a truly different relation, or it may be that there was some systematic error in the calculation of steam flow rates. If, for example, the inlet heaters were heating the end piece enough that water was turned to steam after it passed the inlet thermocouples and entered the core, the result would be underestimated inlet steam quality. This bears further investigation with particular focus on the region of water saturation between 50% and 75%.

From the graphs, residual water saturation appears to be around 30%, and residual steam saturation appears to be around 10%. Residual steam saturation is hard to determine since the drainage tests began with an initial water saturation of about 100%.

The data points from the low-pressure stages are not consistent with the rest of the data. This may be due to an actual effect of pressure on relative permeability, but it is more likely due to two other factors. The low-pressure flow tests are also the flow tests with highest water saturation, and low pressure gradients are more significantly disturbed by fluctuations and inaccuracies in the pressure transducers.

5.8. Data analysis methods

The values for mean relative permeability across the core were calculated by taking the harmonic average of the relative permeabilities for all points along the core, then plotting against the mean saturation across the core. This accounted for the varying viscosity and density, whereas averaging the temperature and viscosity and calculating relative permeability based on the overall pressure drop would not have done so. The data was originally calculated considering all data points, then considering only the interior data points (ignoring the data points closest to the inlet and outlet). There was no noticeable difference in the appearance of the averaged data; while the capillary end effect may create anomalous outlying points on a graph of all data, these points will not significantly alter the average of the data. In Figure 5.8b, the same method was used, but only the values for saturation and relative permeability between ports 2 and 5 were considered.

Averaging the saturation across the core does not account for the flow tests in which the saturation varied across the half of the core nearest the outlet, as was the case for approximately half of the drainage tests. This problem was to be eliminated by only considering ports 2 through 5. However, even when the whole core was considered and averaged, the points from these tests did not diverge from the data trends, as the relationship between relative permeability and saturation is nearly linear over the relatively small range of saturation seen in those tests.

Data were also compiled for the relative permeability as measured at each individual pressure port. The shapes of the relative permeability graph were similar throughout, though each pressure port had different endpoints. The lack of high water saturation values in the latter part of the core limited the data available in those sections, and the graphs overall did not reveal any abnormalities in any of the interior pressure ports.

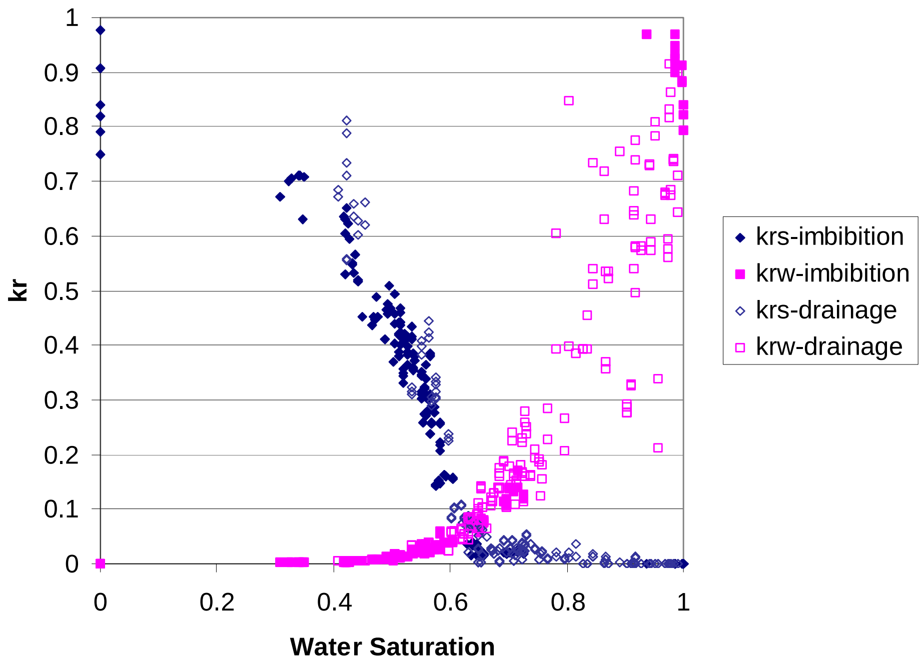

(a) All data

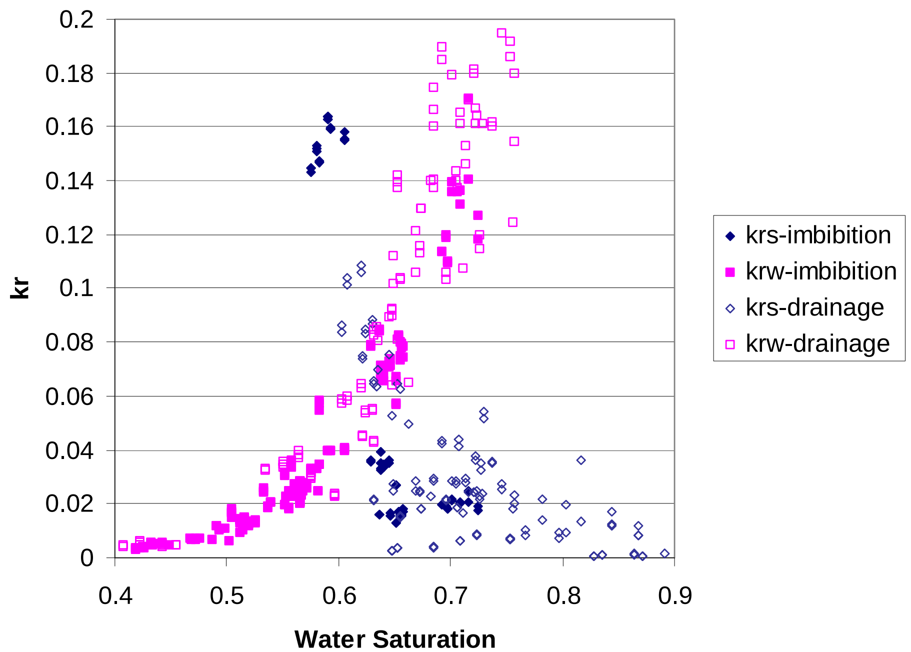

(b) Close-up of area of intersection

Figure 5.5: All data points.

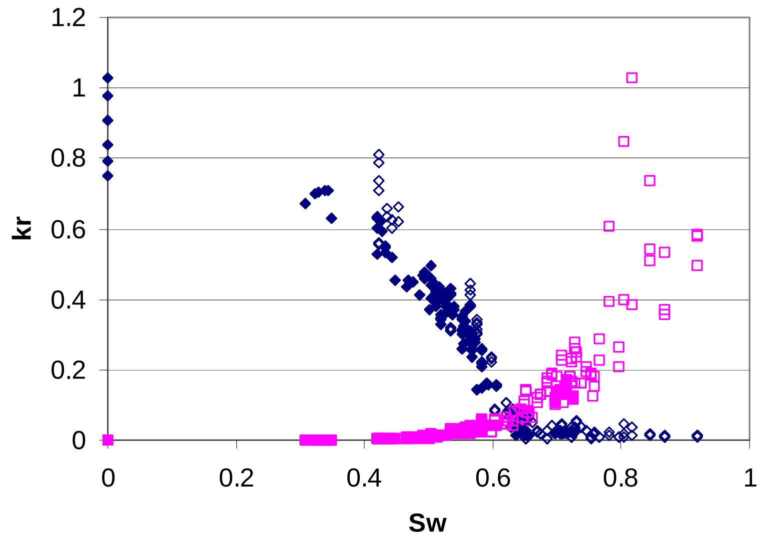

(a) All data

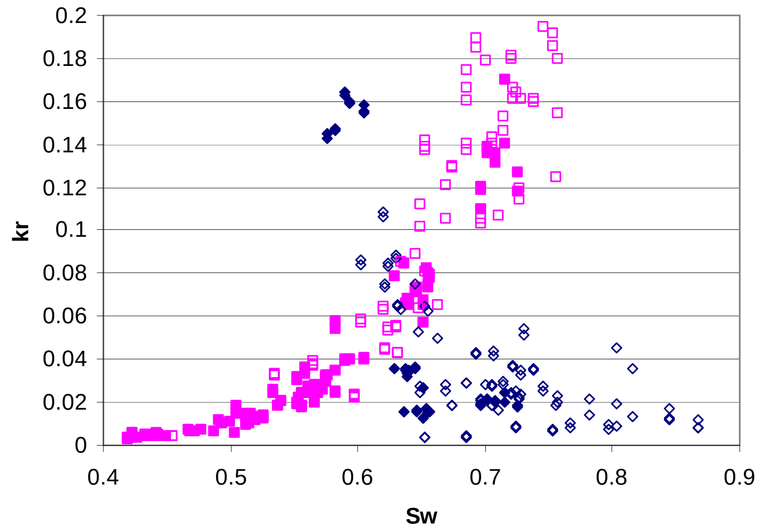

(b) Close-up of area of intersection

Figure 5.6: Interior data points, 15 psi pressure drop. Legend as in Figure 5.5.

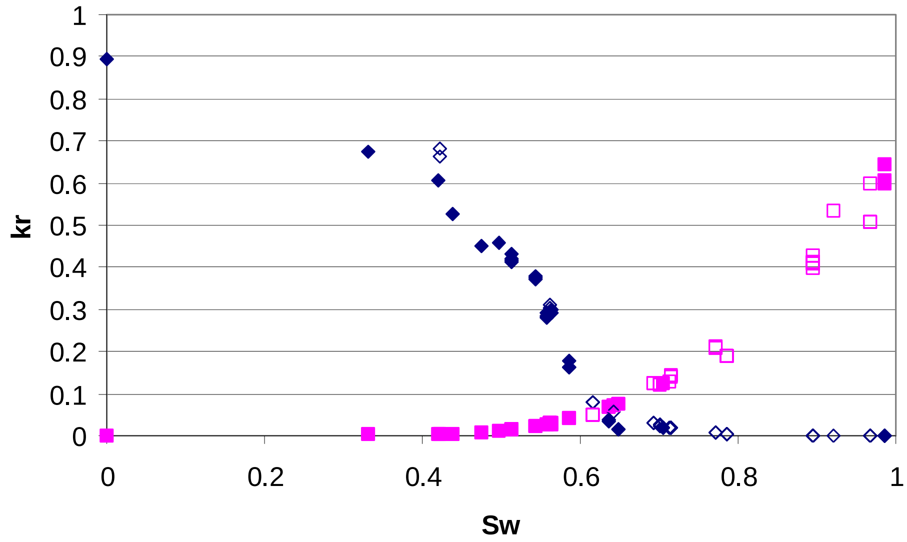

(a) All flow tests

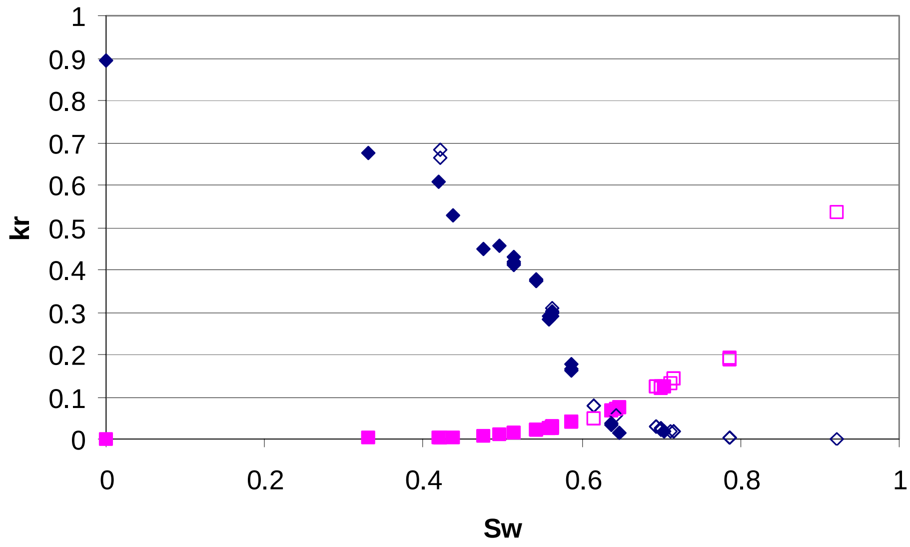

(b) Constant pressure flow tests

Figure 5.7: Harmonic means.

Legend as in Figure 5.5.

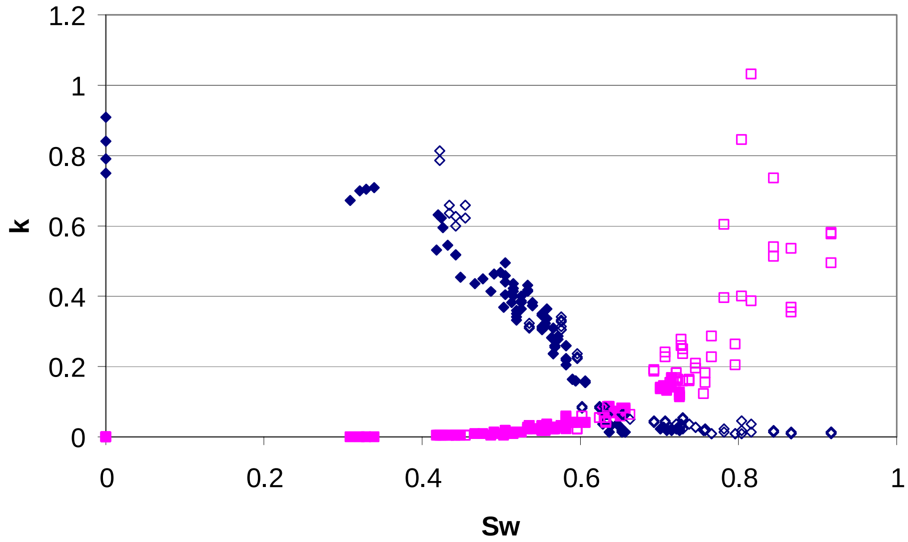

(a) Ports 2-5

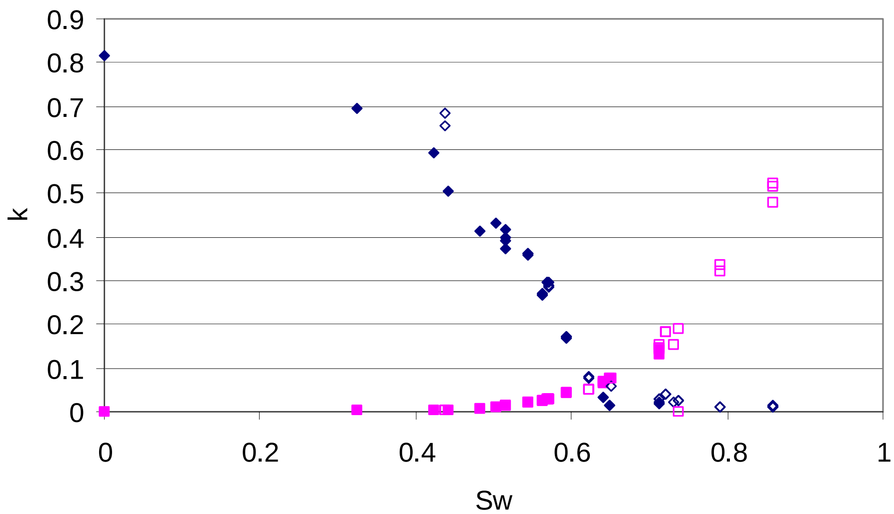

(b) Average of ports 2-5

Figure 5.8: Experiments conducted at constant saturation and ~15 psi pressure drop Legend as in Figure 5.5.

5.9. Comparison to previous results

Figure 5.9 shows the results of this experiment (the harmonic average data presented in Figure 5.7a) compared with previous results obtained by Satik (1998) and Mahiya (1999). The general trend of the data is similar in shape. Data from this experiment agrees more with the Mahiya data in fixing the point of intersection of steam and water relative permeability at S_w = 0.65, rather than the 0.55 determined by Satik. Relative permeabilities were, overall, lower for water flow and higher for steam flow than in the previous experiments.

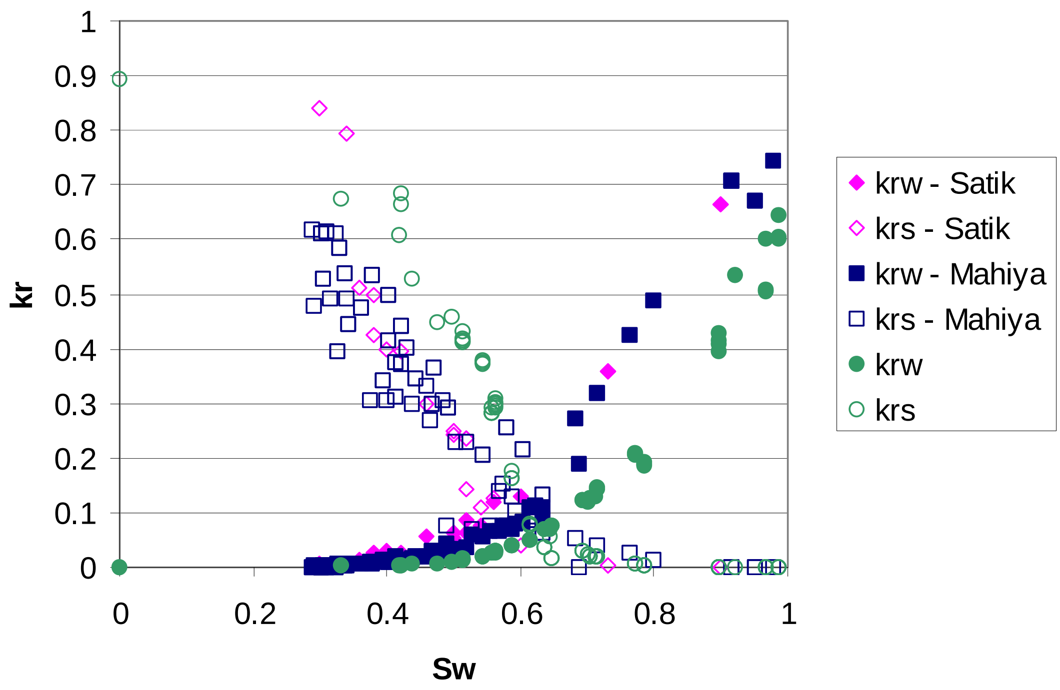

Figure 5.9: Comparison of results with previous experiments.

6. Conclusion

This experiment built on the methodology developed in previous experiments to determine steam-water relative permeability at constant pressure gradient. Heat flux was controlled successfully to maintain adiabatic conditions within the core, though concerns remain about excessive heat gain or loss through the inlet. A constant pressure gradient was maintained in most cases, though maintaining a constant pressure gradient at high water flow rates continues to be a challenge.

A comprehensive data set was compiled. Pressure, temperature, and saturation were measured and recorded and used to calculate relative permeability. The data were then analyzed in a number of ways, and several representations of the steam-water relative permeability relations were presented.

The relative permeability relations suggested by this study support a Corey-type profile for water relative permeability, though they suggest otherwise for steam relative permeability. As in previous experiments, residual water saturation of this core was found to be in the vicinity of 30%. Residual steam saturation was more difficult to determine but apparently near 10%. The steam phase slip factor has a significant effect on the relative permeability. If not considered, it will increase the apparent relative permeability of the steam phase by 20-40%.

This relative permeability experiment focused on a specific Berea sandstone core under a pressure gradient of 15 psi across 43 cm, with an inlet temperature of 120 °C. As geothermal reservoirs tend to be of a composition different than sandstone, with temperatures in excess of 120 °C, these results are not directly applicable to geothermal reservoir engineering in their current form. However, they do provide important insights into the general behavior of steam and water in two-phase flow, which should be similar in form if not in detail to the flow properties of steam and water under geothermal conditions. The experimental methodology established should prove useful for expanding this experiment to include geothermal reservoir material.

For the immediate future, it is our hope that subsequent investigations involve similar experiments at a different pressure gradient, to evaluate the role of pressure and temperature on relative permeability. Experimentation at a greater pressure gradient may require the development of a different core holder mechanism, while experimentation at a lesser pressure gradient may require more sensitive and precise transducers.

References

Ambusso, W.J., “Experimental Determination of Steam-Water Relative Permeability Relations,” MS thesis, Stanford University, Stanford, California (1996).

Clossman, P.J. and Vinegar, J.J., “Relative Permeability to Steam and Water at Residual Oil in Natural Cores; CT Scan Saturation,” SPE paper 174449.

Corey, A.T., “The Interrelations Between Gas and Oil Relative Permeabilities,” *Producers Monthly* Vol. 19 (1954), pp 38-41.

Li, K. and Horne, R.N., “Accurate Measurement of Steam Flow Properties,” GRC Transactions 23 (1999).

Mahiya, G, “Experimental Measurement Of Steam-Water Relative Permeability,” MS thesis, Stanford University, Stanford, California (1999).

Satik, C., “A Measurement of Steam-Water Relative Permeability,” Proceedings of 23rd Workshop on Geothermal Reservoir Engineering, Stanford University, Stanford, California (1998)

A. CT Values

slice	hot water 3271-3272	hotdry 3274	steam1 3276	flow2 3277	flow3 3278	flow4 3279	flow5b 3280
1	1451	1204	1195	1244	1286	1295	1307
2	1442	1194	1183	1258	1288	1295	1300
3	1447	1200	1189	1272	1294	1301	1307
4	1453	1203	1195	1279	1300	1307	1313
5	1459	1210	1204	1286	1322	1323	1327
5	1457	1209	1203	1284	1306	1311	1320
6	1451	1191	1155	1243	1278	1291	1314
7	1458	1208	1193	1278	1305	1309	1317
8	1451	1203	1192	1277	1302	1307	1316
9	1437	1177	1148	1241	1274	1277	1294
10	1440	1191	1184	1270	1291	1296	1306
11	1456	1198	1198	1285	1305	1309	1318
12	1435	1143	1154	1250	1274	1276	1291
13	1454	1196	1196	1285	1305	1308	1318
14	1451	1193	1194	1281	1301	1305	1314
15	1454	1197	1195	1284	1303	1307	1318
16	1454	1192	1192	1283	1302	1305	1315
17	1446	1189	1187	1277	1296	1300	1308
18	1443	1193	1188	1277	1295	1299	1309
19	1447	1198	1192	1281	1300	1304	1312

slice	flow6 3281	flow7 3282	flow8 3283	flow9 3284	flow9b 3286	flow10 3287	flow11 3289
1	1314	1317	1329	1332	1333	1347	1351
2	1307	1312	1322	1324	1321	1335	1343
3	1312	1315	1322	1329	1332	1336	1348
4	1318	1323	1329	1335	1339	1345	1358
5	1333	1337	1345	1349	1350	1355	1366
5	1327	1329	1337	1341	1341	1349	1360
6	1312	1312	1322	1325	1333	1339	1354
7	1324	1328	1338	1341	1342	1349	1360
8	1323	1327	1333	1338	1340	1346	1358
9	1302	1304	1313	1315	1313	1320	1332
10	1313	1316	1322	1328	1331	1335	1347
11	1324	1328	1335	1344	1342	1351	1364
12	1297	1302	1308	1312	1315	1319	1336
13	1324	1328	1336	1340	1341	1347	1361
14	1320	1325	1332	1337	1340	1344	1359
15	1323	1328	1355	1338	1338	1345	1360
16	1321	1329	1333	1336	1340	1344	1360
17	1315	1322	1326	1331	1332	1335	1351
18	1314	1321	1326	1333	1333	1340	1354
19	1318	1322	1328	1332	1334	1336	1351

slice	flow12 3290	flow13 3291	flow14 3293	drain2 3295	drain3 3296	drain4 3297	drain5 3311	drain6 3312
1	1356	1376	1451	1433	1442	1427	1386	1405
2	1347	1364	1441	1427	1435	1423	1379	1405
3	1348	1370	1443	1430	1438	1422	1377	1419
4	1358	1375	1450	1442	1442	1435	1382	1429
5	1368	1388	1455	1453	1448	1443	1389	1442
5	1364	1388	1452	1449	1446	1438	1389	1435
6	1352	1371	1448	1434	1436	1427	1381	1415
7	1362	1384	1453	1443	1440	1432	1392	1420
8	1360	1379	1451	1445	1431	1427	1389	1413
9	1339	1348	1434	1421	1414	1398	1359	1385
10	1353	1366	1440	1439	1425	1415	1375	1404
11	1367	1380	1456	1455	1446	1442	1387	1417
12	1337	1350	1435	1422	1419	1403	1353	1367
13	1365	1377	1454	1453	1440	1432	1380	1374
14	1362	1373	1451	1449	1428	1426	1376	1372
15	1365	1374	1454	1449	1428	1426	1375	1369
16	1362	1375	1454	1449	1422	1420	1370	1364
17	1354	1367	1446	1442	1411	1409	1360	1355
18	1359	1366	1438	1443	1404	1408	1363	1357
19	1356	1367	1420	1436	1398	1398	1351	1353

slice	drain7 3313	drain8 3314	drain9 3315	drain10 3316	drain11 3317	drain12 3318	drain13 3319	drain14 3320
1	1409	1384	1378	1376	1354	1344	1332	1255
2	1400	1369	1364	1361	1342	1334	1323	1268
3	1401	1371	1368	1364	1348	1340	1326	1293
4	1405	1380	1376	1372	1355	1348	1333	1301
5	1409	1392	1388	1394	1369	1360	1342	1319
5	1414	1390	1380	1385	1364	1356	1337	1306
6	1390	1375	1376	1389	1356	1348	1343	1301
7	1405	1387	1380	1384	1364	1355	1341	1303
8	1392	1382	1376	1379	1360	1353	1339	1303
9	1374	1351	1356	1362	1340	1331	1319	1283
10	1387	1371	1366	1369	1351	1342	1329	1294
11	1398	1380	1380	1385	1365	1359	1346	1309
12	1367	1345	1352	1357	1339	1333	1316	1277
13	1393	1372	1376	1380	1364	1357	1342	1305
14	1388	1366	1374	1378	1361	1354	1341	1303
15	1387	1365	1374	1377	1361	1355	1341	1304
16	1382	1363	1371	1376	1361	1355	1340	1303
17	1374	1354	1365	1368	1354	1347	1333	1296
18	1375	1355	1368	1370	1358	1350	1337	1299
19	1366	1347	1355	1358	1346	1340	1324	1289

B. Data and Calculations

		steam1				
inlet X	I_w (Amperes)	V_w (Volts)	I_s (Amperes)	V_s (Volts)	m_w (kg/s)	m_s (kg/s)
1.00E+00	0.000	0	1.225	96.2	0.00E+00	3.83E-05

	distance (cm)	T (°C)	P(psig)	P(bars)	μ_s (cp)	μ_w (cp)
ST inlet	0	130.322	13.908	1.972		
HW inlet	0	126.968	14.209	1.993		
1	3.5	155.380	13.089	1.916	0.01292	0.2345
2	8.5	148.532	11.626	1.815	0.01286	0.2381
3	13.5	141.960	10.198	1.716	0.01280	0.2419
4	18.5	136.496	8.827	1.622	0.01274	0.2459
5	23.5	128.876	7.085	1.502	0.01266	0.2514
6	28.5	112.771	5.768	1.411	0.01259	0.2559
7	33.5	115.602	4.316	1.311	0.01252	0.2614
8	38.5	109.824	2.475	1.184	0.01242	0.2693
outlet	43.5	102.736	0.481	1.046	0.01230	0.2792

	ρ_s (kg/m^3)	ρ_w (kg/m^3)	k_{rs}	k_{rw}	S_{st}	k_{rs} (corr)
1	1.0844	944.03	1.6858	0.0000	1.000	1.3630
2	1.0309	945.37	0.9882	0.0000	1.000	0.7906
3	0.9784	946.73	1.0618	0.0000	1.000	0.8398
4	0.9279	948.09	1.1607	0.0000	1.000	0.9070
5	0.8635	949.89	0.9755	0.0000	1.000	0.7492
6	0.8145	951.31	1.3609	0.0000	1.000	1.0299
7	0.7604	952.95	1.3145	0.0000	1.000	0.9766
8	0.6913	955.16	1.1312	0.0000	1.000	0.8178
outlet	0.6159	957.72	1.1608	0.0000	1.000	0.8098
mean			1.1727	0.0000	1.000	0.8929

flow2

inlet X	I_w (Amperes)	V_w (Volts)	I_s (Amperes)	V_s (Volts)	m_w (kg/s)	m_s (kg/s)
8.89E-01	0.000	0	1.200	94.3	4.17E-06	3.33E-05

	distance (cm)	T (°C)	P(psig)	P(bars)	μ_s (cp)	μ_w (cp)
ST inlet	0	130.772	15.561	2.086		
HW inlet	0	127.320	15.286	2.067		
1	3.5	120.616	14.466	2.011	0.01297	0.2313
2	8.5	119.209	13.082	1.915	0.01292	0.2345
3	13.5	117.491	11.583	1.812	0.01286	0.2382
4	18.5	115.879	10.100	1.710	0.01279	0.2422
5	23.5	113.927	8.568	1.604	0.01273	0.2467
6	28.5	111.169	6.966	1.494	0.01265	0.2518
7	33.5	109.152	5.052	1.362	0.01256	0.2586
8	38.5	106.921	3.250	1.237	0.01246	0.2659
outlet	43.5	102.472	0.430	1.043	0.01230	0.2795

	ρ_s (kg/m^3)	ρ_w (kg/m^3)	k_{rs}	k_{rw}	S_{st}	k_{rs} (corr)
1	1.1346	942.80	1.0521	0.0038	0.809	0.8585
2	1.0841	944.03	0.8676	0.0023	0.694	0.7015
3	1.0293	945.41	0.8399	0.0021	0.678	0.6717
4	0.9748	946.83	0.8920	0.0022	0.691	0.7050
5	0.9184	948.35	0.9118	0.0021	0.671	0.7108
6	0.8591	950.02	0.9267	0.0021	0.661	0.7108
7	0.7879	952.11	0.8395	0.0018	0.658	0.6297
8	0.7204	954.21	0.9677	0.0019	0.653	0.7081
outlet	0.6140	957.79	0.7158	0.0013	0.651	0.4989
mean			0.8813	0.0020	0.670	0.6759

flow3

inlet X	I_w (Amperes)	V_w (Volts)	I_s (Amperes)	V_s (Volts)	m_w (kg/s)	m_s (kg/s)
8.00E-01	0.000	0	1.130	88.6	7.50E-06	3.00E-05

	distance (cm)	T (°C)	P(psig)	P(bars)	μ_s (cp)	μ_w (cp)
ST inlet	0	125.436	15.368	2.073		
HW inlet	0	122.653	14.960	2.045		
1	3.5	120.344	14.249	1.996	0.01296	0.2318
2	8.5	118.823	12.835	1.898	0.01291	0.2351
3	13.5	116.807	11.105	1.779	0.01284	0.2395
4	18.5	115.070	9.497	1.668	0.01277	0.2439
5	23.5	113.056	7.912	1.559	0.01270	0.2487
6	28.5	110.226	6.269	1.445	0.01262	0.2542
7	33.5	108.257	4.439	1.319	0.01253	0.2610
8	38.5	105.817	2.637	1.195	0.01243	0.2686
outlet	43.5	101.439	0.126	1.022	0.01228	0.2812

	ρ_s (kg/m^3)	ρ_w (kg/m^3)	k_{rs}	k_{rw}	S_{st}	k_{rs} (corr)
1	1.1267	942.99	0.9325	0.0078	0.645	0.7598
2	1.0751	944.26	0.7702	0.0040	0.594	0.6216
3	1.0118	945.86	0.6653	0.0033	0.575	0.5301
4	0.9526	947.42	0.7561	0.0036	0.581	0.5945
5	0.8941	949.02	0.8128	0.0037	0.574	0.6296
6	0.8332	950.76	0.8363	0.0037	0.579	0.6365
7	0.7650	952.81	0.8118	0.0034	0.581	0.6041
8	0.6974	954.96	0.8972	0.0035	0.580	0.6503
outlet	0.6024	958.20	0.7362	0.0027	0.578	0.5099
mean			0.7945	0.0037	0.580	0.6078

flow4

inlet X	I_w (Amperes)	V_w (Volts)	I_s (Amperes)	V_s (Volts)	m_w (kg/s)	m_s (kg/s)
7.00E-01	0.000	0	1.060	83.3	1.05E-05	2.45E-05

	distance (cm)	T (°C)	P(psig)	P(bars)	μ_s (cp)	μ_w (cp)
ST inlet	0	128.011	14.673	2.025		
HW inlet	0	125.368	14.208	1.993		
1	3.5	119.604	13.613	1.952	0.01294	0.2333
2	8.5	118.018	12.208	1.855	0.01288	0.2366
3	13.5	116.106	10.528	1.739	0.01281	0.2410
4	18.5	114.465	9.001	1.634	0.01275	0.2454
5	23.5	112.457	7.495	1.530	0.01268	0.2500
6	28.5	109.698	5.924	1.422	0.01260	0.2554
7	33.5	107.844	4.219	1.304	0.01251	0.2618
8	38.5	105.609	2.522	1.187	0.01242	0.2691
outlet	43.5	101.867	0.202	1.027	0.01228	0.2808

	ρ_s (kg/m^3)	ρ_w (kg/m^3)	k_{rs}	k_{rw}	S_{st}	k_{rs} (corr)
1	1.1035	943.55	0.8193	0.0132	0.609	0.6648
2	1.0522	944.83	0.6455	0.0057	0.567	0.5187
3	0.9906	946.41	0.5704	0.0048	0.558	0.4524
4	0.9344	947.91	0.6619	0.0054	0.551	0.5181
5	0.8787	949.46	0.7098	0.0056	0.557	0.5475
6	0.8204	951.14	0.7245	0.0054	0.568	0.5492
7	0.7567	953.07	0.7186	0.0051	0.567	0.5332
8	0.6930	955.10	0.7825	0.0053	0.566	0.5662
outlet	0.6053	958.10	0.6479	0.0040	0.563	0.4494
mean			0.6904	0.0055	0.562	0.5267

flow5b

inlet X	I_w (Amperes)	V_w (Volts)	I_s (Amperes)	V_s (Volts)	m_w (kg/s)	m_s (kg/s)
6.00E-01	0.000	0	0.968	75.7	1.33E-05	2.00E-05

	distance (cm)	T (°C)	P(psig)	P(bars)	μ_s (cp)	μ_w (cp)
ST inlet	0	122.322	14.230	1.994		
HW inlet	0	119.683	14.014	1.979		
1	3.5	119.383	13.342	1.933	0.01293	0.2339
2	8.5	117.944	11.971	1.839	0.01287	0.2372
3	13.5	115.951	10.276	1.722	0.01280	0.2417
4	18.5	114.076	8.694	1.613	0.01273	0.2463
5	23.5	112.127	7.189	1.509	0.01266	0.2510
6	28.5	109.418	5.601	1.399	0.01259	0.2565
7	33.5	107.519	3.947	1.285	0.01250	0.2629
8	38.5	105.383	2.335	1.174	0.01241	0.2700
outlet	43.5	101.518	0.362	1.038	0.01229	0.2799

	ρ_s (kg/m^3)	ρ_w (kg/m^3)	k_{rs}	k_{rw}	S_{st}	k_{rs} (corr)
1	1.0936	943.80	0.8049	0.0149	0.563	0.6520
2	1.0435	945.05	0.5441	0.0074	0.545	0.4365
3	0.9813	946.66	0.4655	0.0061	0.533	0.3684
4	0.9230	948.22	0.5274	0.0066	0.497	0.4116
5	0.8673	949.78	0.5867	0.0071	0.513	0.4511
6	0.8083	951.50	0.5930	0.0068	0.524	0.4479
7	0.7465	953.38	0.6123	0.0067	0.528	0.4526
8	0.6860	955.33	0.6788	0.0071	0.532	0.4896
outlet	0.6114	957.88	0.6162	0.0060	0.527	0.4289
mean			0.5904	0.0071	0.525	0.4499

flow6

inlet X	I_w (Amperes)	V_w (Volts)	I_s (Amperes)	V_s (Volts)	m_w (kg/s)	m_s (kg/s)
5.00E-01	0.000	0	0.980	76.4	2.08E-05	2.08E-05

	distance (cm)	T (°C)	P(psig)	P(bars)	μ_s (cp)	μ_w (cp)
ST inlet	0	123.915	14.565	2.017		
HW inlet	0	120.223	14.129	1.987		
1	3.5	119.649	13.415	1.938	0.01293	0.2337
2	8.5	118.139	12.080	1.846	0.01288	0.2370
3	13.5	116.232	10.373	1.728	0.01281	0.2415
4	18.5	114.370	8.774	1.618	0.01274	0.2460
5	23.5	112.379	7.266	1.514	0.01267	0.2508
6	28.5	109.551	5.651	1.403	0.01259	0.2564
7	33.5	107.713	4.018	1.290	0.01250	0.2626
8	38.5	105.581	2.406	1.179	0.01241	0.2696
outlet	43.5	101.753	0.448	1.044	0.01230	0.2794

	ρ_s (kg/m^3)	ρ_w (kg/m^3)	k_{rs}	k_{rw}	S_{st}	k_{rs} (corr)
1	1.0963	943.73	0.6460	0.0219	0.535	0.5235
2	1.0475	944.95	0.5801	0.0118	0.522	0.4657
3	0.9849	946.56	0.4799	0.0094	0.510	0.3801
4	0.9260	948.14	0.5419	0.0102	0.488	0.4233
5	0.8702	949.70	0.6081	0.0110	0.486	0.4680
6	0.8102	951.44	0.6061	0.0105	0.501	0.4580
7	0.7492	953.30	0.6439	0.0106	0.506	0.4764
8	0.6887	955.24	0.7045	0.0110	0.507	0.5088
outlet	0.6146	957.77	0.6437	0.0094	0.506	0.4488
mean			0.5991	0.0111	0.503	0.4577

flow7

inlet X	I_w (Amperes)	V_w (Volts)	I_s (Amperes)	V_s (Volts)	m_w (kg/s)	m_s (kg/s)
4.10E-01	0.000	0	1.012	79.3	3.00E-05	2.08E-05

	distance (cm)	T (°C)	P(psig)	P(bars)	μ_s (cp)	μ_w (cp)
ST inlet	0	126.375	15.667	2.093		
HW inlet	0	121.298	15.254	2.065		
1	3.5	120.522	14.526	2.015	0.01297	0.2312
2	8.5	119.086	13.150	1.920	0.01292	0.2344
3	13.5	116.927	11.299	1.792	0.01284	0.2390
4	18.5	115.003	9.565	1.673	0.01277	0.2437
5	23.5	112.903	7.896	1.558	0.01270	0.2487
6	28.5	109.940	6.172	1.439	0.01261	0.2545
7	33.5	108.039	4.300	1.310	0.01252	0.2615
8	38.5	105.585	2.519	1.187	0.01242	0.2691
outlet	43.5	101.500	0.466	1.045	0.01230	0.2793

	ρ_s (kg/m^3)	ρ_w (kg/m^3)	k_{rs}	k_{rw}	S_{st}	k_{rs} (corr)
1	1.1368	942.75	0.6300	0.0306	0.523	0.5142
2	1.0866	943.97	0.5443	0.0164	0.507	0.4403
3	1.0189	945.68	0.4291	0.0124	0.495	0.3424
4	0.9551	947.35	0.4858	0.0135	0.480	0.3822
5	0.8935	949.04	0.5364	0.0142	0.474	0.4154
6	0.8296	950.87	0.5557	0.0141	0.485	0.4225
7	0.7598	952.97	0.5545	0.0133	0.488	0.4119
8	0.6929	955.10	0.6341	0.0144	0.478	0.4588
outlet	0.6153	957.74	0.6133	0.0129	0.484	0.4277
mean			0.5458	0.0147	0.487	0.4191

flow8

inlet X	I_w (Amperes)	V_w (Volts)	I_s (Amperes)	V_s (Volts)	m_w (kg/s)	m_s (kg/s)
3.02E-01	0.000	0	0.963	75.2	4.17E-05	1.80E-05

	distance (cm)	T (°C)	P(psig)	P(bars)	μ_s (cp)	μ_w (cp)
ST inlet	0	124.279	15.019	2.049		
HW inlet	0	120.387	14.628	2.022		
1	3.5	120.986	13.961	1.976	0.01295	0.2325
2	8.5	119.517	12.692	1.888	0.01290	0.2355
3	13.5	117.579	10.982	1.770	0.01283	0.2398
4	18.5	115.763	9.342	1.657	0.01276	0.2444
5	23.5	113.657	7.727	1.546	0.01269	0.2493
6	28.5	110.702	6.066	1.431	0.01261	0.2549
7	33.5	108.700	4.184	1.302	0.01251	0.2620
8	38.5	106.141	2.322	1.173	0.01241	0.2700
outlet	43.5	101.843	0.148	1.023	0.01228	0.2811

	ρ_s (kg/m^3)	ρ_w (kg/m^3)	k_{rs}	k_{rw}	S_{st}	k_{rs} (corr)
1	1.1162	943.24	0.5968	0.0466	0.477	0.4854
2	1.0699	944.39	0.5172	0.0248	0.474	0.4170
3	1.0072	945.98	0.4055	0.0187	0.467	0.3228
4	0.9469	947.57	0.4473	0.0198	0.444	0.3512
5	0.8873	949.22	0.4820	0.0205	0.449	0.3727
6	0.8256	950.99	0.5005	0.0203	0.460	0.3801
7	0.7554	953.11	0.4791	0.0184	0.434	0.3553
8	0.6855	955.35	0.5292	0.0191	0.463	0.3817
outlet	0.6033	958.17	0.5095	0.0170	0.463	0.3531
mean			0.4912	0.0210	0.457	0.3752

flow9

inlet X	I_w (Amperes)	V_w (Volts)	I_s (Amperes)	V_s (Volts)	m_w (kg/s)	m_s (kg/s)
2.05E-01	0.320	25	0.932	73	5.43E-05	1.40E-05

	distance (cm)	T (°C)	P(psig)	P(bars)	μ_s (cp)	μ_w (cp)
ST inlet	0	126.680	15.540	2.085		
HW inlet	0	121.365	15.831	2.105		
1	3.5	120.821	14.839	2.036	0.01298	0.2305
2	8.5	119.445	13.535	1.946	0.01293	0.2334
3	13.5	117.554	11.759	1.824	0.01286	0.2378
4	18.5	115.568	10.046	1.706	0.01279	0.2424
5	23.5	113.538	8.410	1.593	0.01272	0.2471
6	28.5	110.540	6.644	1.471	0.01264	0.2529
7	33.5	108.468	4.652	1.334	0.01254	0.2601
8	38.5	105.671	2.640	1.195	0.01243	0.2686
outlet	43.5	101.491	0.337	1.036	0.01229	0.2800

	ρ_s (kg/m^3)	ρ_w (kg/m^3)	k_{rs}	k_{rw}	S_{st}	k_{rs} (corr)
1	1.1482	942.47	0.6828	0.0405	0.465	0.5584
2	1.1007	943.62	0.3815	0.0312	0.456	0.3094
3	1.0357	945.25	0.2960	0.0233	0.448	0.2371
4	0.9728	946.88	0.3250	0.0246	0.434	0.2567
5	0.9125	948.51	0.3607	0.0262	0.432	0.2808
6	0.8471	950.36	0.3576	0.0248	0.436	0.2734
7	0.7729	952.57	0.3447	0.0225	0.444	0.2573
8	0.6975	954.95	0.3749	0.0230	0.447	0.2718
outlet	0.6104	957.91	0.3701	0.0209	0.441	0.2574
mean			0.3692	0.0254	0.442	0.2830

flow9b

inlet X	I_w (Amperes)	V_w (Volts)	I_s (Amperes)	V_s (Volts)	m_w (kg/s)	m_s (kg/s)
2.05E-01	0.000	0	0.960	75.4	5.43E-05	1.40E-05

	distance (cm)	T (°C)	P(psig)	P(bars)	μ_s (cp)	μ_w (cp)
ST inlet	0	127.460	14.717	2.028		
HW inlet	0	124.261	13.667	1.956		
1	3.5	119.579	13.579	1.949	0.01293	0.2333
2	8.5	118.306	12.353	1.865	0.01289	0.2363
3	13.5	116.484	10.684	1.750	0.01282	0.2406
4	18.5	114.699	9.106	1.641	0.01275	0.2451
5	23.5	112.658	7.585	1.536	0.01268	0.2497
6	28.5	109.617	5.952	1.424	0.01260	0.2553
7	33.5	107.784	4.092	1.295	0.01251	0.2623
8	38.5	105.182	2.246	1.168	0.01241	0.2704
outlet	43.5	101.030	0.114	1.021	0.01227	0.2812

	ρ_s (kg/m^3)	ρ_w (kg/m^3)	k_{rs}	k_{rw}	S_{st}	k_{rs} (corr)
1	1.1023	943.58	0.4365	0.4617	0.461	0.3541
2	1.0575	944.70	0.4208	0.0335	0.456	0.3385
3	0.9963	946.26	0.3264	0.0250	0.442	0.2592
4	0.9382	947.81	0.3646	0.0269	0.418	0.2857
5	0.8820	949.36	0.4002	0.0284	0.428	0.3090
6	0.8214	951.11	0.3978	0.0270	0.434	0.3017
7	0.7520	953.21	0.3786	0.0243	0.439	0.2804
8	0.6826	955.44	0.4168	0.0252	0.438	0.3002
outlet	0.6020	958.22	0.4049	0.0226	0.437	0.2804
mean			0.3914	0.0294	0.437	0.2985

flow10

inlet X	I_w (Amperes)	V_w (Volts)	I_s (Amperes)	V_s (Volts)	m_w (kg/s)	m_s (kg/s)
9.09E-02	0.473	37	0.853	66.8	9.17E-05	9.17E-06

	distance (cm)	T (°C)	P(psig)	P(bars)	μ_s (cp)	μ_w (cp)
ST inlet	0	128.509	16.068	2.121		
HW inlet	0	120.015	16.322	2.139		
1	3.5	121.474	15.914	2.110	0.01302	0.2282
2	8.5	120.538	14.669	2.025	0.01298	0.2309
3	13.5	118.933	12.949	1.906	0.01291	0.2348
4	18.5	117.075	11.196	1.785	0.01284	0.2392
5	23.5	114.862	9.411	1.662	0.01276	0.2442
6	28.5	111.604	7.296	1.516	0.01267	0.2507
7	33.5	108.940	5.005	1.358	0.01256	0.2588
8	38.5		2.652	1.196	0.01243	0.2685
outlet	43.5		0.273	1.032	0.01229	0.2804

	ρ_s (kg/m^3)	ρ_w (kg/m^3)	k_{rs}	k_{rw}	S_{st}	k_{rs} (corr)
1	1.1873	941.55	1.9741	0.1646	0.406	1.6248
2	1.1420	942.62	0.2530	0.0545	0.422	0.2067
3	1.0793	944.15	0.1928	0.0401	0.417	0.1557
4	1.0151	945.78	0.2000	0.0400	0.395	0.1595
5	0.9495	947.51	0.2088	0.0400	0.407	0.1640
6	0.8713	949.67	0.1906	0.0346	0.410	0.1467
7	0.7861	952.17	0.1933	0.0329	0.417	0.1449
8	0.6979	954.94	0.2098	0.0331	0.424	0.1521
outlet	0.6080	958.00	0.2354	0.0341	0.420	0.1636
mean			0.2315	0.0413	0.414	0.1777

flow11

inlet X	I_w (Amperes)	V_w (Volts)	I_s (Amperes)	V_s (Volts)	m_w (kg/s)	m_s (kg/s)
1.19E-02	0.864	68.1	0.688	54.3	1.67E-04	2.00E-06

	distance (cm)	T (°C)	P(psig)	P(bars)	μ_s (cp)	μ_w (cp)
ST inlet	0	129.384	16.811	2.172		
HW inlet	0	123.661	17.389	2.212		
1	3.5	122.358	16.053	2.120	0.01303	0.2279
2	8.5	120.694	14.481	2.012	0.01297	0.2313
3	13.5	118.463	12.278	1.860	0.01288	0.2365
4	18.5	116.344	10.398	1.730	0.01281	0.2414
5	23.5	113.954	8.602	1.606	0.01273	0.2466
6	28.5	110.538	6.614	1.469	0.01264	0.2530
7	33.5	108.536	4.524	1.325	0.01253	0.2606
8	38.5		2.532	1.188	0.01242	0.2690
outlet	43.5		0.093	1.020	0.01227	0.2814

	ρ_s (kg/m^3)	ρ_w (kg/m^3)	k_{rs}	k_{rw}	S_{st}	k_{rs} (corr)
1	1.1923	941.43	0.0872	0.0913	0.391	0.0718
2	1.1352	942.79	0.0440	0.0786	0.383	0.0359
3	1.0547	944.77	0.0335	0.0573	0.372	0.0270
4	0.9858	946.54	0.0418	0.0684	0.349	0.0331
5	0.9196	948.32	0.0466	0.0730	0.362	0.0363
6	0.8460	950.39	0.0454	0.0675	0.354	0.0347
7	0.7681	952.71	0.0472	0.0660	0.360	0.0352
8	0.6934	955.08	0.0544	0.0713	0.363	0.0394
outlet	0.6012	958.25	0.0506	0.0607	0.363	0.0350
mean			0.0472	0.0693	0.363	0.0363

flow12

inlet X	I_w (Amperes)	V_w (Volts)	I_s (Amperes)	V_s (Volts)	m_w (kg/s)	m_s (kg/s)
4.98E-03	0.960	79.1	0.630	49.9	2.00E-04	1.00E-06

	distance (cm)	T (°C)	P(psig)	P(bars)	μ_s (cp)	μ_w (cp)
ST inlet	0	128.929	18.245	2.271		
HW inlet	0	122.564	19.000	2.323		
1	3.5	123.589	17.423	2.215	0.01307	0.2251
2	8.5	121.840	15.690	2.095	0.01301	0.2286
3	13.5	119.473	13.467	1.942	0.01293	0.2336
4	18.5	117.535	11.555	1.810	0.01285	0.2383
5	23.5	115.209	9.674	1.680	0.01278	0.2434
6	28.5	111.898	7.503	1.531	0.01268	0.2500
7	33.5	109.347	5.205	1.372	0.01257	0.2580
8	38.5		2.923	1.215	0.01244	0.2673
outlet	43.5		0.152	1.024	0.01228	0.2810

	ρ_s (kg/m^3)	ρ_w (kg/m^3)	k_{rs}	k_{rw}	S_{st}	k_{rs} (corr)
1	1.2420	940.29	0.0387	0.0918	0.371	0.0321
2	1.1792	941.74	0.0193	0.0847	0.375	0.0158
3	1.0982	943.69	0.0160	0.0673	0.364	0.0130
4	1.0283	945.44	0.0198	0.0797	0.348	0.0158
5	0.9592	947.25	0.0214	0.0826	0.343	0.0169
6	0.8790	949.45	0.0201	0.0734	0.347	0.0155
7	0.7936	951.94	0.0208	0.0713	0.345	0.0157
8	0.7081	954.61	0.0233	0.0742	0.353	0.0170
outlet	0.6034	958.17	0.0222	0.0640	0.343	0.0154
mean			0.0213	0.0757	0.352	0.0165

flow13

inlet X	I_w (Amperes)	V_w (Volts)	I_s (Amperes)	V_s (Volts)	m_w (kg/s)	m_s (kg/s)
3.74E-03	1.038	82.6	0.628	49.77	2.67E-04	1.00E-06

	distance (cm)	T (°C)	P(psig)	P(bars)	μ_s (cp)	μ_w (cp)
ST inlet	0	124.907	15.330	2.070		
HW inlet	0	118.459	15.702	2.096		
1	3.5	119.524	14.256	1.996	0.01296	0.2318
2	8.5	118.586	13.080	1.915	0.01292	0.2345
3	13.5	117.137	11.477	1.805	0.01285	0.2385
4	18.5	115.528	9.962	1.700	0.01279	0.2426
5	23.5	113.379	8.455	1.596	0.01272	0.2470
6	28.5	110.611	6.669	1.473	0.01264	0.2528
7	33.5	108.480	4.662	1.335	0.01254	0.2601
8	38.5		2.670	1.197	0.01243	0.2684
outlet	43.5		0.210	1.028	0.01228	0.2807

	ρ_s (kg/m³)	ρ_w (kg/m³)	k_{rs}	k_{rw}	S_{st}	k_{rs} (corr)
1	1.1270	942.98	0.0324	0.1371	0.293	0.0264
2	1.0841	944.03	0.0306	0.1703	0.300	0.0248
3	1.0254	945.51	0.0236	0.1269	0.284	0.0189
4	0.9698	946.96	0.0263	0.1364	0.275	0.0208
5	0.9142	948.47	0.0279	0.1394	0.292	0.0217
6	0.8480	950.33	0.0252	0.1201	0.299	0.0193
7	0.7733	952.56	0.0244	0.1097	0.304	0.0182
8	0.6986	954.92	0.0270	0.1138	0.303	0.0196
outlet	0.6056	958.09	0.0249	0.0960	0.308	0.0173
mean			0.0267	0.1247	0.295	0.0204

flow14

inlet X	I_w (Amperes)	V_w (Volts)	I_s (Amperes)	V_s (Volts)	m_w (kg/s)	m_s (kg/s)
4.69E-06	1.720	133	0.000	0	7.50E-04	0.00E+00

	distance (cm)	T (°C)	P(psig)	P(bars)	μ_s (cp)	μ_w (cp)
ST inlet	0	90.630	8.684	1.612		
HW inlet	0	81.489	9.120	1.642		
1	3.5	102.347	6.113	1.435	0.01261	0.2547
2	8.5	100.911	5.444	1.389	0.01258	0.2571
3	13.5	99.266	4.781	1.343	0.01254	0.2596
4	18.5	99.371	4.072	1.294	0.01251	0.2624
5	23.5	98.922	3.477	1.253	0.01247	0.2649
6	28.5	97.312	3.018	1.221	0.01245	0.2669
7	33.5	99.214	2.238	1.168	0.01240	0.2704
8	38.5		2.118	1.159	0.01240	0.2710
outlet	43.5		0.385	1.040	0.01229	0.2797

	ρ_s (kg/m^3)	ρ_w (kg/m^3)	k_{rs}	k_{rw}	S_{st}	k_{rs} (corr)
1	0.8274	950.93	0.0001	0.2020	0.000	0.0000
2	0.8025	951.67	0.0002	0.9159	0.010	0.0002
3	0.7777	952.42	0.0003	0.9325	0.016	0.0002
4	0.7512	953.24	0.0002	0.8806	0.015	0.0002
5	0.7289	953.94	0.0003	1.0585	0.003	0.0002
6	0.7117	954.49	0.0004	1.3815	0.000	0.0003
7	0.6823	955.45	0.0002	0.8229	0.000	0.0002
8	0.6778	955.60	0.0016	5.3591	0.000	0.0012
outlet	0.6123	957.85	0.0001	0.3822	0.063	0.0001
mean			0.0002	0.6458	0.013	0.0001

drain2

inlet X	I_w (Amperes)	V_w (Volts)	I_s (Amperes)	V_s (Volts)	m_w (kg/s)	m_s (kg/s)
7.30E-06	0.750	57.4	0.708	54.2	1.67E-04	6.92E-05

	distance (cm)	T (°C)	P(psig)	P(bars)	μ_s (cp)	μ_w (cp)
ST inlet	0	98.677	3.887	1.281		
HW inlet	0	95.819	3.349	1.244		
1	3.5	95.763	2.301	1.172	0.01241	0.2701
2	8.5	96.108	2.001	1.151	0.01239	0.2715
3	13.5	95.390	1.646	1.127	0.01237	0.2732
4	18.5	95.245	1.290	1.102	0.01235	0.2750
5	23.5	94.829	1.065	1.087	0.01233	0.2761
6	28.5	93.221	0.835	1.071	0.01232	0.2773
7	33.5	94.460	0.555	1.052	0.01230	0.2788
8	38.5		0.313	1.035	0.01229	0.2801
outlet	43.5		0.287	1.033	0.01229	0.2803

	ρ_s (kg/m^3)	ρ_w (kg/m^3)	k_{rs}	k_{rw}	S_{st}	k_{rs} (corr)
1	0.6847	955.37	0.0001	0.1924	0.070	0.0001
2	0.6734	955.75	0.0003	0.6753	0.062	0.0002
3	0.6600	956.20	0.0003	0.5740	0.033	0.0002
4	0.6466	956.66	0.0003	0.5758	0.057	0.0002
5	0.6380	956.95	0.0004	0.9146	0.027	0.0003
6	0.6293	957.25	0.0004	0.8983	0.025	0.0003
7	0.6187	957.62	0.0004	0.7416	0.010	0.0003
8	0.6095	957.95	0.0004	0.8618	0.017	0.0003
outlet	0.6085	957.98	0.0040	8.0251	0.022	0.0028
mean			0.0003	0.6001	0.032	0.0002

drain3

inlet X	I_w (Amperes)	V_w (Volts)	I_s (Amperes)	V_s (Volts)	m_w (kg/s)	m_s (kg/s)
2.31E-05	1.068	81.9	0.000	0	2.67E-04	0.00E+00

	distance (cm)	T (°C)	P(psig)	P(bars)	μ_s (cp)	μ_w (cp)
ST inlet	0	94.907	4.088	1.295		
HW inlet	0	88.979	4.169	1.301		
1	3.5	99.147	3.746	1.272	0.01249	0.2638
2	8.5	97.873	2.678	1.198	0.01243	0.2684
3	13.5	96.554	2.367	1.176	0.01241	0.2698
4	18.5	96.418	1.973	1.149	0.01239	0.2717
5	23.5	95.893	1.688	1.130	0.01237	0.2730
6	28.5	93.989	1.389	1.109	0.01235	0.2745
7	33.5	95.498	0.953	1.079	0.01233	0.2767
8	38.5		0.352	1.038	0.01229	0.2799
outlet	43.5		0.315	1.035	0.01229	0.2801

	ρ_s (kg/m^3)	ρ_w (kg/m^3)	k_{rs}	k_{rw}	S_{st}	k_{rs} (corr)
1	0.7390	953.62	0.0007	0.5273	0.035	0.0005
2	0.6989	954.91	0.0003	0.2122	0.031	0.0002
3	0.6872	955.29	0.0011	0.7323	0.043	0.0008
4	0.6724	955.78	0.0009	0.5817	0.059	0.0006
5	0.6616	956.14	0.0012	0.8079	0.072	0.0009
6	0.6503	956.53	0.0012	0.7740	0.048	0.0008
7	0.6338	957.09	0.0008	0.5347	0.081	0.0006
8	0.6110	957.89	0.0006	0.3921	0.129	0.0004
outlet	0.6096	957.94	0.0101	6.3732	0.173	0.0071
mean			0.0008	0.5357	0.079	0.0006

drain4

inlet X	I_w (Amperes)	V_w (Volts)	I_s (Amperes)	V_s (Volts)	m_w (kg/s)	m_s (kg/s)
4.20E-05	1.140	82.2	0.000	0	2.42E-04	0.00E+00

	distance (cm)	T (°C)	P(psig)	P(bars)	μ_s (cp)	μ_w (cp)
ST inlet	0	101.682	4.679	1.336		
HW inlet	0	95.564	4.977	1.356		
1	3.5	105.317	3.771	1.273	0.01249	0.2637
2	8.5	104.220	3.631	1.264	0.01248	0.2642
3	13.5	103.597	3.009	1.221	0.01245	0.2669
4	18.5	103.445	2.865	1.211	0.01244	0.2676
5	23.5	102.930	2.543	1.189	0.01242	0.2690
6	28.5	102.089	1.787	1.136	0.01238	0.2725
7	33.5	102.016	1.496	1.116	0.01236	0.2740
8	38.5		1.456	1.114	0.01236	0.2742
outlet	43.5		0.422	1.042	0.01229	0.2795

	ρ_s (kg/m^3)	ρ_w (kg/m^3)	k_{rs}	k_{rw}	S_{st}	k_{rs} (corr)
1	0.7400	953.59	0.0004	0.1675	0.094	0.0003
2	0.7347	953.76	0.0037	1.4462	0.085	0.0027
3	0.7114	954.50	0.0009	0.3285	0.069	0.0006
4	0.7059	954.68	0.0038	1.4222	0.090	0.0027
5	0.6938	955.07	0.0017	0.6392	0.108	0.0012
6	0.6653	956.02	0.0008	0.2756	0.084	0.0005
7	0.6543	956.39	0.0020	0.7194	0.097	0.0014
8	0.6528	956.44	0.0145	5.2369	0.136	0.0103
outlet	0.6137	957.80	0.0006	0.2063	0.165	0.0004
mean			0.0011	0.4085	0.104	0.0008

drain5

inlet X	I_w (Amperes)	V_w (Volts)	I_s (Amperes)	V_s (Volts)	m_w (kg/s)	m_s (kg/s)
3.20E-03	1.307	95.2	0.000	0	2.78E-04	0.00E+00

	distance (cm)	T (°C)	P(psig)	P(bars)	μ_s (cp)	μ_w (cp)
ST inlet	0	106.914	13.014	1.911		
HW inlet	0	106.957	14.507	2.013		
1	3.5	118.598	12.926	1.904	0.01291	0.2349
2	8.5	117.556	12.109	1.848	0.01288	0.2369
3	13.5	116.237	10.731	1.753	0.01282	0.2405
4	18.5	114.754	9.624	1.677	0.01277	0.2436
5	23.5	113.481	8.409	1.593	0.01272	0.2472
6	28.5	110.794	6.767	1.480	0.01264	0.2524
7	33.5	108.900	5.010	1.359	0.01256	0.2587
8	38.5		2.728	1.201	0.01243	0.2682
outlet	43.5		0.253	1.031	0.01228	0.2805

	ρ_s (kg/m^3)	ρ_w (kg/m^3)	k_{rs}	k_{rw}	S_{st}	k_{rs} (corr)
1	1.0784	944.17	0.0204	0.1320	0.254	0.0165
2	1.0486	944.92	0.0405	0.2575	0.257	0.0325
3	0.9980	946.22	0.0251	0.1547	0.272	0.0199
4	0.9573	947.30	0.0324	0.1949	0.243	0.0255
5	0.9125	948.51	0.0309	0.1799	0.254	0.0240
6	0.8517	950.23	0.0243	0.1357	0.280	0.0186
7	0.7863	952.16	0.0245	0.1298	0.295	0.0183
8	0.7008	954.84	0.0209	0.1033	0.326	0.0152
outlet	0.6072	958.03	0.0220	0.0992	0.345	0.0153
mean			0.0256	0.1419	0.284	0.0195

drain6

inlet X	I_w (Amperes)	V_w (Volts)	I_s (Amperes)	V_s (Volts)	m_w (kg/s)	m_s (kg/s)
5.84E-04	1.530	111.5	0.000	0	4.17E-04	

	distance (cm)	T (°C)	P(psig)	P(bars)	μ_s (cp)	μ_w (cp)
ST inlet	0	110.698	14.577	2.018		
HW inlet	0	107.011	16.260	2.134		
1	3.5	119.885	14.254	1.996	0.01296	0.2318
2	8.5	118.443	13.716	1.959	0.01294	0.2330
3	13.5	117.516	12.836	1.898	0.01291	0.2351
4	18.5	116.562	12.220	1.856	0.01288	0.2366
5	23.5	115.853	11.846	1.830	0.01287	0.2376
6	28.5	115.024	9.906	1.696	0.01279	0.2428
7	33.5	112.237	7.573	1.535	0.01268	0.2498
8	38.5		3.786	1.274	0.01249	0.2636
outlet	43.5	101.353	0.282	1.033	0.01229	0.2803

	ρ_s (kg/m^3)	ρ_w (kg/m^3)	k_{rs}	k_{rw}	S_{st}	k_{rs} (corr)
1	1.1269	942.99	0.0042	0.1543	0.180	0.0034
2	1.1073	943.46	0.0160	0.5781	0.126	0.0130
3	1.0752	944.25	0.0100	0.3563	0.082	0.0081
4	1.0526	944.82	0.0146	0.5120	0.133	0.0118
5	1.0389	945.17	0.0244	0.8463	0.156	0.0195
6	0.9677	947.02	0.0050	0.1664	0.197	0.0040
7	0.8816	949.38	0.0045	0.1420	0.315	0.0035
8	0.7405	953.57	0.0033	0.0919	0.347	0.0024
outlet	0.6083	957.99	0.0042	0.1052	0.353	0.0029
mean			0.0061	0.1891	0.214	0.0047

drain7

inlet X	I_w (Amperes)	V_w (Volts)	I_s (Amperes)	V_s (Volts)	m_w (kg/s)	m_s (kg/s)
8.27E-04	1.186	86.3	0.000	0	2.50E-04	0.00E+00

	distance (cm)	T (°C)	P(psig)	P(bars)	μ_s (cp)	μ_w (cp)
ST inlet	0	107.927	7.802	1.551		
HW inlet	0	101.670	9.311	1.655		
1	3.5	111.823	7.733	1.546	0.01269	0.2493
2	8.5	110.548	7.540	1.533	0.01268	0.2499
3	13.5	110.030	6.566	1.466	0.01263	0.2531
4	18.5	109.361	6.052	1.431	0.01261	0.2549
5	23.5	108.713	5.336	1.381	0.01257	0.2575
6	28.5	107.416	4.254	1.307	0.01252	0.2617
7	33.5	106.214	3.340	1.244	0.01247	0.2655
8	38.5		2.042	1.154	0.01239	0.2713
outlet	43.5		0.419	1.042	0.01229	0.2796

	ρ_s (kg/m^3)	ρ_w (kg/m^3)	k_{rs}	k_{rw}	S_{st}	k_{rs} (corr)
1	0.8875	949.21	0.0057	0.1257	0.164	0.0044
2	0.8803	949.41	0.0466	1.0301	0.170	0.0360
3	0.8442	950.44	0.0096	0.2065	0.184	0.0073
4	0.8251	951.00	0.0186	0.3939	0.203	0.0141
5	0.7985	951.79	0.0137	0.2854	0.218	0.0103
6	0.7580	953.03	0.0095	0.1917	0.233	0.0071
7	0.7238	954.10	0.0118	0.2300	0.247	0.0086
8	0.6750	955.70	0.0088	0.1652	0.276	0.0063
outlet	0.6135	957.80	0.0077	0.1358	0.292	0.0054
mean			0.0104	0.2103	0.228	0.0078

drain8

inlet X	I_w (Amperes)	V_w (Volts)	I_s (Amperes)	V_s (Volts)	m_w (kg/s)	m_s (kg/s)
5.56E-03	1.275	92.8	0.000	0	2.67E-04	0.00E+00

	distance (cm)	T (°C)	P(psig)	P(bars)	μ_s (cp)	μ_w (cp)
ST inlet	0	114.345	14.126	1.987		
HW inlet	0	107.168	15.797	2.102		
1	3.5	119.878	13.992	1.978	0.01295	0.2324
2	8.5	118.826	13.155	1.920	0.01292	0.2343
3	13.5	117.695	11.909	1.834	0.01287	0.2374
4	18.5	116.245	10.687	1.750	0.01282	0.2406
5	23.5	114.898	9.572	1.673	0.01277	0.2437
6	28.5	112.397	7.839	1.554	0.01269	0.2489
7	33.5	109.976	5.718	1.407	0.01259	0.2561
8	38.5		3.013	1.221	0.01245	0.2669
outlet	43.5		0.300	1.034	0.01229	0.2802

	ρ_s (kg/m^3)	ρ_w (kg/m^3)	k_{rs}	k_{rw}	S_{st}	k_{rs} (corr)
1	1.1174	943.22	0.0288	0.1095	0.262	0.0234
2	1.0868	943.97	0.0637	0.2378	0.288	0.0515
3	1.0412	945.11	0.0445	0.1617	0.270	0.0357
4	0.9964	946.26	0.0472	0.1669	0.262	0.0375
5	0.9554	947.35	0.0538	0.1850	0.278	0.0423
6	0.8914	949.10	0.0368	0.1214	0.307	0.0285
7	0.8127	951.37	0.0328	0.1018	0.331	0.0248
8	0.7115	954.50	0.0290	0.0829	0.351	0.0212
outlet	0.6090	957.96	0.0333	0.0865	0.369	0.0232
mean			0.0383	0.1239	0.307	0.0294

drain9

inlet X	I_w (Amperes)	V_w (Volts)	I_s (Amperes)	V_s (Volts)	m_w (kg/s)	m_s (kg/s)
4.67E-03	1.275	92.3	0.000	0	2.50E-04	0.00E+00

	distance (cm)	T (°C)	P(psig)	P(bars)	μ_s (cp)	μ_w (cp)
ST inlet	0	113.334	12.917	1.904		
HW inlet	0	107.015	14.998	2.047		
1	3.5	118.722	12.893	1.902	0.01291	0.2350
2	8.5	117.723	12.104	1.848	0.01288	0.2369
3	13.5	116.057	10.505	1.738	0.01281	0.2411
4	18.5	114.637	9.237	1.650	0.01276	0.2447
5	23.5	112.749	7.863	1.555	0.01269	0.2489
6	28.5	110.287	5.955	1.424	0.01260	0.2553
7	33.5	108.056	4.488	1.323	0.01253	0.2608
8	38.5		2.663	1.197	0.01243	0.2685
outlet	43.5		0.370	1.039	0.01229	0.2798

	ρ_s (kg/m^3)	ρ_w (kg/m^3)	k_{rs}	k_{rw}	S_{st}	k_{rs} (corr)
1	1.0772	944.20	0.0201	0.0890	0.285	0.0162
2	1.0484	944.93	0.0549	0.2391	0.304	0.0441
3	0.9897	946.44	0.0286	0.1199	0.293	0.0226
4	0.9431	947.68	0.0376	0.1532	0.274	0.0295
5	0.8923	949.07	0.0365	0.1436	0.286	0.0283
6	0.8215	951.11	0.0284	0.1058	0.295	0.0215
7	0.7668	952.75	0.0393	0.1404	0.304	0.0293
8	0.6983	954.92	0.0344	0.1159	0.315	0.0249
outlet	0.6117	957.87	0.0309	0.0959	0.327	0.0215
mean			0.0322	0.1235	0.300	0.0247

drain10

inlet X	I_w (Amperes)	V_w (Volts)	I_s (Amperes)	V_s (Volts)	m_w (kg/s)	m_s (kg/s)
3.47E-03	1.137	82.9	0.000	0	2.00E-04	0.00E+00

	distance (cm)	T (°C)	P(psig)	P(bars)	μ_s (cp)	μ_w (cp)
ST inlet	0	107.724	9.874	1.694		
HW inlet	0	106.222	11.742	1.823		
1	3.5	115.448	9.997	1.703	0.01279	0.2425
2	8.5	114.155	9.081	1.639	0.01275	0.2451
3	13.5	112.739	7.814	1.552	0.01269	0.2490
4	18.5	111.283	6.821	1.484	0.01265	0.2523
5	23.5	109.801	5.836	1.416	0.01260	0.2557
6	28.5	107.750	4.295	1.309	0.01252	0.2615
7	33.5	106.265	3.359	1.245	0.01247	0.2654
8	38.5		2.138	1.161	0.01240	0.2709
outlet	43.5	101.473	0.452	1.044	0.01230	0.2794

	ρ_s (kg/m^3)	ρ_w (kg/m^3)	k_{rs}	k_{rw}	S_{st}	k_{rs} (corr)
1	0.9710	946.93	0.0159	0.0884	0.293	0.0125
2	0.9373	947.83	0.0312	0.1702	0.317	0.0244
3	0.8905	949.13	0.0236	0.1248	0.284	0.0183
4	0.8537	950.17	0.0314	0.1611	0.244	0.0240
5	0.8171	951.24	0.0329	0.1645	0.272	0.0249
6	0.7596	952.98	0.0225	0.1073	0.276	0.0167
7	0.7245	954.08	0.0386	0.1791	0.289	0.0283
8	0.6786	955.57	0.0315	0.1399	0.299	0.0226
outlet	0.6148	957.76	0.0249	0.1043	0.318	0.0174
mean			0.0263	0.1302	0.288	0.0198

drain11

inlet X	I_w (Amperes)	V_w (Volts)	I_s (Amperes)	V_s (Volts)	m_w (kg/s)	m_s (kg/s)
1.84E-02	1.088	79.3	0.000	0	1.50E-04	0.00E+00

	distance (cm)	T (°C)	P(psig)	P(bars)	μ_s	μ_w
ST inlet	0	104.974	14.758	2.031		
HW inlet	0	111.299	15.492	2.081		
1	3.5	119.050	13.096	1.916	0.01292	0.2345
2	8.5	117.370	11.789	1.826	0.01286	0.2377
3	13.5	115.553	10.039	1.705	0.01279	0.2424
4	18.5	113.809	8.597	1.606	0.01273	0.2466
5	23.5	111.744	7.142	1.506	0.01266	0.2512
6	28.5	109.200	5.264	1.376	0.01257	0.2578
7	33.5	107.172	3.891	1.282	0.01250	0.2632
8	38.5		2.330	1.174	0.01241	0.2700
outlet	43.5		0.387	1.040	0.01229	0.2797

	ρ_s (kg/m^3)	ρ_w (kg/m^3)	k_{rs}	k_{rw}	S_{st}	k_{rs} (corr)
1	1.0847	944.02	0.0415	0.0462	0.379	0.0335
2	1.0368	945.22	0.0792	0.0857	0.385	0.0635
3	0.9726	946.89	0.0627	0.0651	0.366	0.0496
4	0.9194	948.32	0.0801	0.0803	0.338	0.0625
5	0.8656	949.83	0.0839	0.0809	0.345	0.0645
6	0.7958	951.87	0.0702	0.0642	0.347	0.0528
7	0.7444	953.45	0.1021	0.0895	0.353	0.0754
8	0.6858	955.34	0.0968	0.0806	0.355	0.0698
outlet	0.6123	957.85	0.0863	0.0669	0.365	0.0601
mean			0.0732	0.0705	0.357	0.0561

drain12

inlet X	I_w (Amperes)	V_w (Volts)	I_s (Amperes)	V_s (Volts)	m_w (kg/s)	m_s (kg/s)
3.62E-02	1.040	75.5	0.000	0	1.17E-04	0.00E+00

	distance (cm)	T (°C)	P(psig)	P(bars)	μ_s (cp)	μ_w (cp)
ST inlet	0	111.913	14.896	2.040		
HW inlet	0	113.790	16.317	2.138		
1	3.5	119.855	14.084	1.984	0.01295	0.2322
2	8.5	118.435	12.640	1.885	0.01290	0.2356
3	13.5	116.312	10.648	1.747	0.01282	0.2407
4	18.5	114.531	9.040	1.637	0.01275	0.2453
5	23.5	112.272	7.425	1.525	0.01267	0.2503
6	28.5	109.563	5.414	1.387	0.01258	0.2572
7	33.5	107.360	3.958	1.286	0.01250	0.2629
8	38.5		2.355	1.176	0.01241	0.2699
outlet	43.5	101.275	0.339	1.037	0.01229	0.2800

	ρ_s (kg/m^3)	ρ_w (kg/m^3)	k_{rs}	k_{rw}	S_{st}	k_{rs} (corr)
1	1.1207	943.14	0.0661	0.0375	0.418	0.0538
2	1.0680	944.43	0.1068	0.0587	0.416	0.0860
3	0.9950	946.30	0.0825	0.0434	0.398	0.0655
4	0.9358	947.88	0.1081	0.0547	0.368	0.0847
5	0.8761	949.53	0.1143	0.0555	0.376	0.0881
6	0.8014	951.71	0.0996	0.0457	0.369	0.0751
7	0.7470	953.37	0.1467	0.0644	0.379	0.1085
8	0.6868	955.30	0.1439	0.0599	0.380	0.1039
outlet	0.6105	957.91	0.1275	0.0493	0.392	0.0887
mean			0.1043	0.0507	0.385	0.0803

drain13

inlet X	I_w (Amperes)	V_w (Volts)	I_s (Amperes)	V_s (Volts)	m_w (kg/s)	m_s (kg/s)
1.99E-01	0.964	70.1	0.000	0	8.33E-05	0.00E+00

	distance (cm)	T (°C)	P(psig)	P(bars)	μ_s (cp)	μ_w (cp)
ST inlet	0	105.792	15.470	2.080		
HW inlet	0	113.521	16.843	2.175		
1	3.5	120.488	14.557	2.017	0.01297	0.2311
2	8.5	118.727	13.023	1.911	0.01291	0.2347
3	13.5	116.434	10.801	1.758	0.01282	0.2403
4	18.5	114.475	9.056	1.638	0.01275	0.2452
5	23.5	112.177	7.379	1.522	0.01267	0.2504
6	28.5	109.571	5.378	1.384	0.01257	0.2574
7	33.5	107.351	3.918	1.283	0.01250	0.2631
8	38.5		2.277	1.170	0.01241	0.2702
outlet	43.5	100.944	0.364	1.038	0.01229	0.2799

	ρ_s (kg/m^3)	ρ_w (kg/m^3)	k_{rs}	k_{rw}	S_{st}	k_{rs} (corr)
1	1.1379	942.72	0.2496	0.0217	0.465	0.2038
2	1.0820	944.09	0.3895	0.0327	0.464	0.3148
3	1.0006	946.15	0.2888	0.0231	0.465	0.2295
4	0.9364	947.86	0.3906	0.0299	0.403	0.3059
5	0.8744	949.58	0.4327	0.0318	0.425	0.3333
6	0.8000	951.75	0.3933	0.0273	0.425	0.2962
7	0.7455	953.42	0.5749	0.0382	0.433	0.4248
8	0.6838	955.40	0.5536	0.0348	0.436	0.3989
outlet	0.6115	957.88	0.5261	0.0308	0.449	0.3661
mean			0.3931	0.0291	0.438	0.3033

drain14

inlet X	I_w (Amperes)	V_w (Volts)	I_s (Amperes)	V_s (Volts)	m_w (kg/s)	m_s (kg/s)
7.72E-01	1.209	88	0.000	0	3.33E-05	0.00E+00

	distance (cm)	T (°C)	P(psig)	P(bars)	μ_s (cp)	μ_w (cp)
ST inlet	0	141.114	12.420	1.870		
HW inlet	0	119.477	12.921	1.904		
1	3.5	118.120	12.216	1.856	0.01288	0.2366
2	8.5	117.022	11.220	1.787	0.01284	0.2392
3	13.5	115.516	9.913	1.697	0.01279	0.2427
4	18.5	113.860	8.513	1.600	0.01272	0.2468
5	23.5	111.992	7.138	1.505	0.01266	0.2512
6	28.5	109.312	5.494	1.392	0.01258	0.2569
7	33.5	107.934	4.194	1.302	0.01251	0.2619
8	38.5		2.733	1.202	0.01243	0.2681
outlet	43.5	102.076	0.690	1.061	0.01231	0.2781

	ρ_s (kg/m^3)	ρ_w (kg/m^3)	k_{rs}	k_{rw}	S_{st}	k_{rs} (corr)
1	1.0525	944.82	1.3510	0.0082	0.766	1.0856
2	1.0160	945.75	0.9875	0.0058	0.634	0.7876
3	0.9680	947.01	0.7865	0.0045	0.578	0.6206
4	0.9163	948.41	0.7719	0.0043	0.546	0.6014
5	0.8654	949.83	0.8280	0.0044	0.558	0.6363
6	0.8043	951.62	0.7404	0.0038	0.566	0.5584
7	0.7558	953.09	0.9911	0.0049	0.578	0.7351
8	0.7010	954.84	0.9448	0.0044	0.578	0.6859
outlet	0.6238	957.44	0.7517	0.0033	0.592	0.5266
mean			0.8758	0.0045	0.579	0.6645